Article

Towards Routine Mapping of Crop Emergence within the Season Using the Harmonized Landsat and Sentinel-2 Dataset

Feng Gao [1,*], **Martha C. Anderson [1]**, **David M. Johnson [2]**, **Robert Seffrin [2]**, **Brian Wardlow [3]**, **Andy Suyker [4]**, **Chunyuan Diao [5]** and **Dawn M. Browning [6]**

1. Hydrology and Remote Sensing Laboratory, U.S. Department of Agriculture, Agricultural Research Service, 10300 Baltimore Avenue, Beltsville, MD 20705, USA; martha.anderson@usda.gov
2. U.S. Department of Agriculture, National Agricultural Statistics Service, 1400 Independence Ave., SW., Washington, DC 20250, USA; david.m.johnson@usda.gov (D.M.J.); robert.seffrin@usda.gov (R.S.)
3. Center for Advanced Land Management Information Technologies, University of Nebraska-Lincoln, 3310 Holdrege St, Lincoln, NE 68583, USA; bwardlow2@unl.edu
4. School of Natural Resources, University of Nebraska-Lincoln, 3310 Holdrege St, Lincoln, NE 68583, USA; asuyker1@unl.edu
5. Department of Geography and Geographic Information Science, University of Illinois at Urbana-Champaign, Urbana, IL 61801, USA; chunyuan@illinois.edu
6. U.S. Department of Agriculture, Agricultural Research Service, Jornada Experimental Range, Las Cruces, NM 88003, USA; dawn.browning@usda.gov
* Correspondence: feng.gao@usda.gov

Abstract: Crop emergence is a critical stage for crop development modeling, crop condition monitoring, and biomass accumulation estimation. Green-up dates (or the start of the season) detected from remote sensing time series are related to, but generally lag, crop emergence dates. In this paper, we refine the within-season emergence (WISE) algorithm and extend application to five Corn Belt states (Iowa, Illinois, Indiana, Minnesota, and Nebraska) using routine harmonized Landsat and Sentinel-2 (HLS) data from 2018 to 2020. Green-up dates detected from the HLS time series were assessed using field observations and near-surface measurements from PhenoCams. Statistical descriptions of green-up dates for corn and soybeans were generated and compared to county-level planting dates and district- to state-level crop emergence dates reported by the National Agricultural Statistics Service (NASS). Results show that emergence dates for corn and soybean can be reliably detected within the season using the HLS time series acquired during the early growing season. Compared to observed crop emergence dates, green-up dates from HLS using WISE were ~3 days later at the field scale (30-m). The mean absolute difference (MAD) was ~7 days and the root mean square error (RMSE) was ~9 days. At the state level, the mean differences between median HLS green-up date and median crop emergence date were within 2 days for 2018–2020. At this scale, MAD was within 4 days, and RMSE was less than 5 days for both corn and soybeans. The R-squares were 0.73 and 0.87 for corn and soybean, respectively. The 2019 late emergence of crops in Corn Belt states (1–4 weeks to five-year average) was captured by HLS green-up date retrievals. This study demonstrates that routine within-season mapping of crop emergence/green-up at the field scale is practicable over large regions using operational satellite data. The green-up map derived from HLS during the growing season provides valuable information on spatial and temporal variability in crop emergence that can be used for crop monitoring and refining agricultural statistics used in broad-scale modeling efforts.

Keywords: crop growth stages; start of the season; green-up; crop progress; crop condition; land surface phenology; remote sensing phenology; time-series analysis; Landsat; Sentinel-2

1. Introduction

Crop emergence is the first indicator of crop success. Crop emergence depends on crop planting date, soil moisture, soil temperature, seed variety, and other factors [1,2]. Under warm soil conditions, crops may emerge within a few days after planting. However,

emergence can take as long as a few weeks under cold soil conditions [3]. At the level of individual fields, crops may fail to emerge and need replanting. Crop emergence dates vary significantly by field and year. Mapping crop emergence at the field scale during the growing season provides critical information for crop growth modeling, crop condition monitoring, biomass accumulation estimation, and yield prediction [4–6].

The United States Department of Agriculture (USDA) National Agricultural Statistics Service (NASS) reports crop emergence dates in Crop Progress reports [7]. Field-level observational data are summarized to the state or agricultural district (multiple counties) level and published weekly. Crop Progress reports offer critical information for crop monitoring at the state and national levels. However, these reports do not include information on spatial variability over the county, district, or state statistical units. Furthermore, for many crop monitoring and management applications, emergence information at the field to sub-field scales will be beneficial.

Remote sensing data have been used to map land surface phenology (LSP) at various spatial resolutions from a few hundred meters to a few meters [8–12]. Green-up dates (or the start of the season) from LSP products can be related to crop emergence dates [13,14]. However, these quantities are different both in definition and extraction approach. Crop emergence is a physiological stage observed from the ground, while the remote sensing green-up date is defined by a certain change or threshold in vegetation indices derived from remote sensing time series [15]. Previous studies revealed that remote sensing green-up dates are generally detected after crop emergence dates. Depending on the algorithm, the lag in detection varies from a few days to a few weeks [13,16,17].

The Moderate-Resolution Imaging Spectroradiometer (MODIS) land cover dynamics data product (MCD12Q2) provides LSP metrics, including green-up dates, at 500 m spatial resolution since 2001 [8]. The Visible Infrared Imaging Radiometer Suite (VIIRS) LSP product inherited the MODIS MCD12Q2 Collection 5 curvature phenology algorithm and has delivered LSP metrics at 500 m spatial resolution (VNP22Q2) since 2013 [9]. However, pixels at 500 m spatial resolution may be constituted of a mixture of different crop types and are typically too coarse to map crop progress at field scale even for large fields in the U.S. [18]. Data fusion approaches have been developed to integrate remote sensing data from multiple sensors for generating remote sensing time series at both high temporal and spatial resolution [19–21], which have been used to extract land surface phenology for crops [13] and forests [22,23]. Recently, the Harmonized Landsat and Sentinel-2 (HLS) dataset [24] has been used to produce yearly LSP at 30 m resolution from 2016 to 2018 for North America through the Multi-Source Land Imaging (MuSLI) project under the National Aeronautics and Space Administration (NASA) Land-Cover and Land-Use Change Program [11].

Remote sensing phenology mapping methods can be categorized as after-season and within-season approaches [15]. After-season approaches produce LSP after the end of the growing season using 2–3 years of remote sensing observations. The MODIS, VIIRS, and HLS phenology products use after-season approaches [8,9,11]. The LSP algorithm of the MODIS product uses three consecutive years of MODIS time-series to produce LSP for the middle year [25]. The VIIRS and HLS LSP algorithms use two years of time-series data, i.e., the year of interest plus 6 months before and after [9,11]. After-season LSP products are usually available 6 months to 1 year after the growing season. These algorithms require information about a complete cycle of vegetation growth and thus can only be implemented retrospectively.

Within-season approaches focus on detecting specific stages using the latest available remote sensing observations and are geared toward near-real-time applications. These algorithms can function using only a partial year of time series [15]. Recently, within-season approaches have been developed to map crop emergence and cover crop termination at the field scale [16,26]. The within-season emergence (WISE) approach was developed using the Vegetation and Environment monitoring New MicroSatellite (VENµS) time series (5-m, 2-day revisit) and validated over the Beltsville Agricultural Research Center (BARC)

experimental fields in Beltsville, MD, during the 2019 growing season. Results show that early crop growth stages can be reliably detected with WISE at the sub-field scale about two weeks after crop emergence. The remote sensing green-up dates were about 4–5 days after crop emergence on average [16]. However, VENμS is a scientific satellite sampling mission that only acquires images over 123 small pre-selected areas (27 by 27 km each) across the globe [27]. It was not designed for operational uses.

This study refines the WISE algorithm to use routine HLS data (30-m, 3–4-day) and applies the algorithm over five states in the U.S. Corn Belt from 2018–2020. This region is intensively cropped and experienced a significant variation, both spatially and temporally, in crop planting and emergence dates during the 3-year period. For example, in 2019, corn planting dates in the U.S. Corn Belt were delayed for 1–4 weeks compared to the 5-year average due to above-normal spring rainfall [7]. The objectives of this paper are to (1) refine the WISE algorithm for operational application over large areas; (2) assess whether HLS data are frequent and sensitive enough for detecting crop emergence within the growing season over a large region; and (3) map green-up dates at 30-m resolution for the Corn Belt states 2018 through 2020.

2. Study Area and Data

2.1. Study Area

Five Corn Belt states (Iowa, Illinois, Indiana, Minnesota, and Nebraska) were selected for this study (Figure 1). These are the top five states in the United States for both corn and soybean production and accounted for more than 50% for corn and 60% for soybean production in the U.S. in 2020 (Table 1). Our study area spans from 37 to 49 degrees north and from 85 to 104 degrees west. The five states include a total area of 815,589 km^2. Spring temperature and soil conditions vary significantly over the study area. Crop emergence dates varied from middle April to late July for corn and from early May to late July for soybeans [7]. In addition to spatial variations, the inter-annual variability of crop emergence dates can be as long as a few weeks, depending on planting conditions and soil temperatures. In 2019, planting dates in Corn Belt were delayed for 1–4 weeks unevenly across the region. This study area provides a large dynamic range of crop emergence dates and is ideal for assessing crop emergence mapping algorithms for operational applications.

2.2. Data Compilation

2.2.1. Phenocam Observation

PhenoCam observations for agricultural sites in Illinois, Iowa, Minnesota, and Nebraska (blue markers in Figure 1) were used to calibrate the WISE algorithm. The PhenoCam network is a cooperative network that collects automated near-surface remote sensing of canopy phenology in the U.S. and other regions [29]. We selected 34 observations from 2017 to 2020, covering corn and soybeans fields at 13 unique PhenoCam sites (Table 2). Among the 13 unique sites, ten are USDA-ARS sites, and 7 of those are the Long-Term Agroecosystem Research (LTAR) member sites [30,31]. At the Mead, NE sites, emergence was also observed in-field through visual scouting [32], T. Arkebauer, personal communication, July 2021. To determine crop emergence dates, the standard PhenoCam 3-day green chromatic coordinate (GCC) data product over the region of interest (ROI) [29,33,34] was first used to infer the green-up inflection period visually during Spring. GCC is the relative brightness of the green band divided by the total brightness of red, green, and blue bands. GCC measures the greenness of canopy within the ROI [34]. Then crop emergence dates were refined by manual examination of PhenoCam photos for each day during the inflection period. The first date that showed the crop emerging in the PhenoCam photo was identified as the crop emergence date. At the Mead sites, field-observed and PhenoCam-derived crop emergence dates were compared. The field-observed emergence dates were a few days earlier than the emergence dates observed from the PhenoCam photos since the photo resolution may not be sufficient to show the first appearance of leaves. It should be noted that the field observations of crop growth stages were conducted

in selected areas of the fields that were not necessarily co-located with the PhenoCam field of view. Different timings of within-field crop emergence could be due to microclimate and other within-field factors. In Table 2, the emergence dates for the PhenoCam sites varied from day 126 (May 6) to 198 (July 17). The number of PhenoCam observations increased from 2017 to 2020 (4, 7, 11, and 12 observations, respectively, in each year). Most of the PhenoCam sites were planted in corn (19 fields) and soybeans (12 fields). The remaining three sites were planted in wheat, sorghum, and grass, respectively. Emergence dates from these sites were also used for comparison with remote sensing green-up dates. We used the PhenoCam observations to tune WISE parameters and assess the WISE algorithm for the HLS time series over the Corn Belt states.
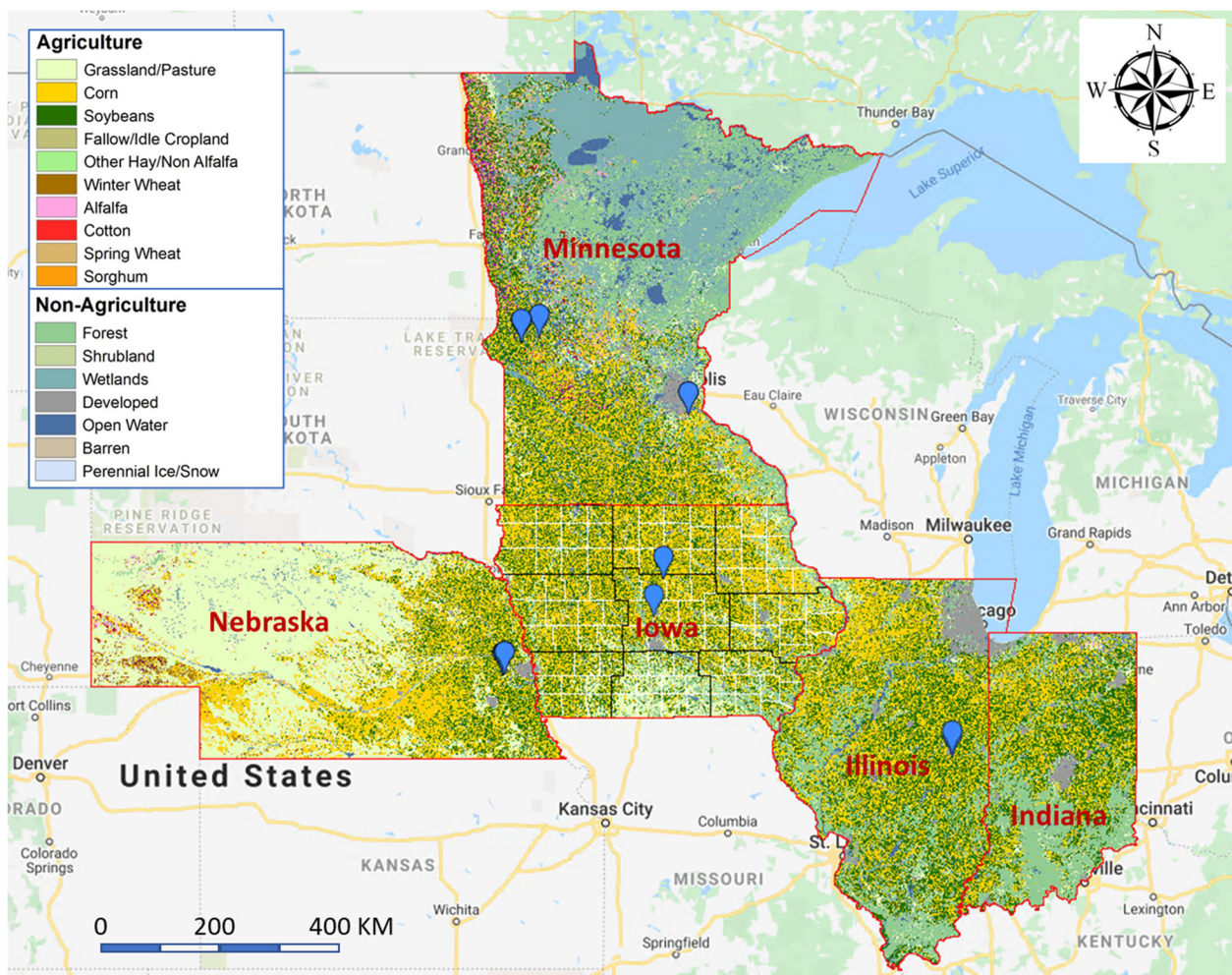

Figure 1. The study area includes five Corn Belt states (Iowa, Illinois, Indiana, Minnesota, and Nebraska, red boundaries), nine agricultural districts in Iowa (NW, NC, NE, WC, C, EC, SW, SC, and SE, black boundaries), 99 counties in Iowa (white boundaries), and 13 unique PhenoCam sites (blue markers) with 34 site-year observations. The map was made in the Google Earth Engine (GEE) and overlaid with the 2020 Cropland Data Layer (CDL). Please note that the scale bar in this figure is approximate from GEE since this map is in Mercator projection.

Table 1. Corn and soybean productions for the top five Corn Belt states in 2020 (NASS Quick Stats [28]).

State	Corn Production (BU)	Portion in US (%)	Ranking in US	Soybean Production (BU)	Portion in US (%)	Ranking in US
Illinois	2,131,200,000	15.03	2	604,750,000	14.62	1
Indiana	981,750,000	6.92	5	329,440,000	7.97	4
Iowa	2,296,200,000	16.19	1	493,960,000	11.94	2
Minnesota	1,441,920,000	10.17	4	359,170,000	8.69	3
Nebraska	1,790,090,000	12.62	3	294,120,000	7.11	5

Table 2. Agricultural PhenoCam sites and emergence (VE) dates (six underlined sites will be investigated in detail in Section 4.2 in terms of varying comparative characteristics between WISE detected green-up and PhenoCam observed crop emergence dates).

State	Name	Latitude	Longitude	Year	VE (Day)	Crop
MN	arsmnswanlake1	45.6845	−95.7997	2018	148	corn
	arsmnswanlake1	45.6845	−95.7997	2019	162	soybean
	arsmnswanlake1	45.6845	−95.7997	2020	149	corn
	arsmorris1	45.6167	−96.1269	2018	147	corn
	arsmorris1	45.6167	−96.1269	2019	170	soybean
	arsmorris1	45.6167	−96.1269	2020	152	corn
	arsmorris2	45.6270	−96.1270	2018	139	wheat
	arsmorris2	45.6270	−96.1270	2019	198	fallow/grass
	arsmorris2	45.6270	−96.1270	2020	148	corn
	rosemountconv	44.6910	−93.0576	2017	159	soybean
	rosemountconv	44.6910	−93.0576	2018	147	corn
	rosemountconv	44.6910	−93.0576	2019	164	soybean
	rosemountconv	44.6910	−93.0576	2020	152	corn
IA	arscolessouth	42.4816	−93.5235	2019	177	soybean
	arscolessouth	42.4816	−93.5235	2020	136	corn
	arscolesnorth	42.4884	−93.5225	2019	164	corn
	arsbrooks10	41.9749	−93.6905	2020	143	soybean
	arsbrooks11	41.9744	−93.6937	2020	126	corn
NE	mead1	41.1651	−96.4766	2017	128	corn
	mead1	41.1651	−96.4766	2018	137	corn
	mead1	41.1651	−96.4766	2019	125	corn
	mead1	41.1651	−96.4766	2020	122	corn
	mead2	41.1649	−96.4701	2017	134	corn
	mead2	41.1649	−96.4701	2018	141	soybean
	mead2	41.1649	−96.4701	2019	131	corn
	mead2	41.1649	−96.4701	2020	141	soybean
	mead3	41.1797	−96.4397	2017	135	corn
	mead3	41.1797	−96.4397	2018	141	soybean
	mead3	41.1797	−96.4397	2019	133	corn
	mead3	41.1797	−96.4397	2020	142	soybean
IL	uiefsorghum	40.0065	−88.2032	2019	144	soybean
	uiefsorghum	40.0065	−88.2032	2020	145	sorghum
	uiefmaize2	40.0628	−88.1961	2019	152	soybean
	uiefmaize2	40.0628	−88.1961	2020	148	corn

2.2.2. HLS Data

We used NASA's Harmonized Landsat and Sentinel-2 (HLS) version 1.4 data in this study. The HLS combines Landsat and Sentinel-2 data to build consistent surface reflectance products at 30-m spatial resolution [24]. To make a consistent HLS data product, Landsat and Sentinel-2 data have been co-registered, atmospherically corrected, Bidirectional Reflectance Distribution Function (BRDF) normalized, and bandpass adjusted. The European Space Agency's (ESA) Sentinel-2 mission comprises a constellation of two polar-orbiting

satellites launched on 23 June 2015 (2A) and 7 March 2017 (2B) [35]. Both satellites (2A and 2B) carry a wide-swath (290 km) Multi-Spectral Instrument (MSI) that acquires 13 multi-spectral bands imagery at 10–60-m spatial resolution. The constellation observes the Earth every 5 days at the equator and more frequently at higher latitudes. In the HLS dataset, the Sentinel-2 data have been resampled to match the Landsat 30-m resolution. The HLS dataset also includes data from Landsat-8, launched on 11 February 2013. Landsat-8 carries the Operational Land Imager (OLI), which observes the entire Earth every 16 days at 30-m resolution [36]. Together, Sentinel-2 and Landsat-8 provide a revisit cycle of 3–4 days over the Earth.

The version 1.4 HLS data are routinely available from the NASA Goddard Space Flight Center (GSFC) [37]. The version 2.0 HLS data have been available from EarthData since late 2021 and focus on forward processing. At the time of manuscript preparation, the backward processing was limited to the Fall of 2020. For this reason, we used version 1.4 in this study. Crop emergence detection is sensitive to available observations in the early growing season [16]; however, Sentinel-2 was not operating at full capacity in the U.S. until late spring in 2017. Thus, we have used HLS data since 2017 to detect green-ups at individual PhenoCam sites collecting observations since 2017, and used HLS images from 2018–2020 for large-areas mapping over the five-state region. Observations of each pixel flagged as clear in HLS data products were used to compute the normalized difference vegetation index (NDVI). In the study area, typical emergence dates vary from middle April to middle July for corn and from early May to late July for soybeans. To include most crop emergence dates, we used HLS data from January 1 to middle August (day 228) of the same year to map crop green-up dates within the season. A total of 109 HLS tiles (Figure 1) from each year were downloaded and processed.

2.2.3. NASS Data

Average crop planting date by county was derived from USDA acreage and compliance determination data collected by the Farm Service Agency [38]. Farmers report this information annually to meet crop insurance rules or participate in other governmental assistance programs. The date was calculated by averaging all records by reported county by the crop of interest and weighted by field acres. County location is the finest level of geography the raw data offer, with the planting date record averaged to preserve record-level confidentiality while still affording a high-quality reference dataset. County-level planting dates were produced for Iowa from 2018–2020 and used in this study.

NASS also publishes weekly crop progress reports, providing the cumulative percentages of crop area at various stages of growth [7]. The state-level summaries are available for all states. In Iowa, the reports include nine agricultural districts (NW, NC, NE, WC, C, EC, SW, SC, SE) [39]. Each district includes multiple counties (Figure 1). In this study, we compare crop emergence dates to remote sensing green-up dates using cumulative percentages and corresponding median values for two statistical units (district-level in Iowa and state-level for five states).

The Cropland Data Layers (CDL) from 2018 to 2020 were used to separate crop types for producing crop-specific statistics. NASS has used multiple medium-resolution satellite datasets to generate the 30-m CDL over the conterminous U.S. every year since 2008 [40]. The national CDL is usually released early the following year after the growing season has ended [41]. Classification accuracies for corn and soybeans in the five states from 2018–2020 were above 90% for producer and user accuracies. Using the CDL, statistical summaries of green-up dates were generated from the 30-m corn and soybean pixels. Please note that while the CDL was used for generating statistics, it is not needed to run the WISE algorithm.

3. Analytical Methods

Green-up dates were detected from the HLS time series using the Moving Average Convergence Divergence (MACD) approach and the WISE algorithm. The remote sensing

green-up dates were compared to crop emergence dates observed at the PhenoCam sites. The crop-specific green-up dates were also summarized and compared to NASS data at various statistic unit scales, including county-level planting dates in Iowa, district-level crop emergence dates in Iowa, and state-level crop emergence dates for five Corn Belt states from 2018 to 2020. Figure 2 illustrates the general workflow of this study.
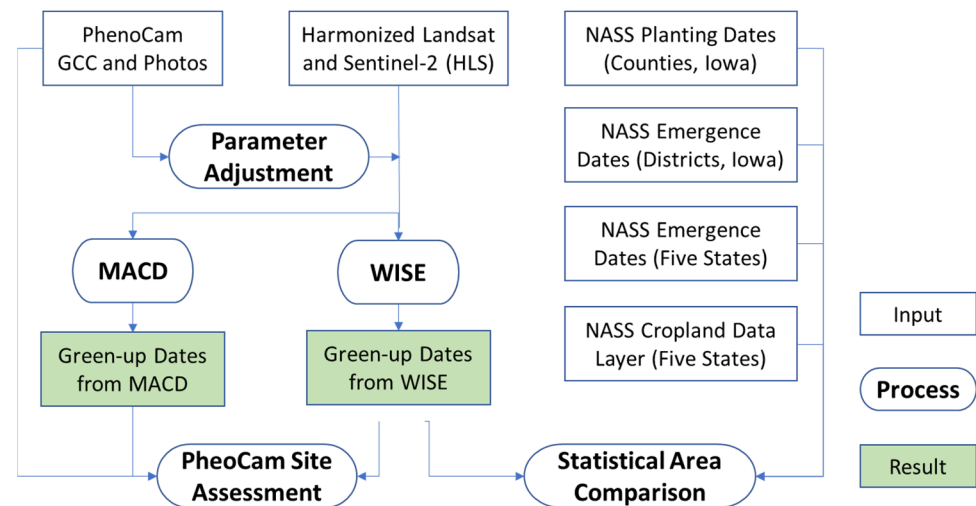

Figure 2. Workflow chart for crop emergence mapping within the season using the Harmonized Landsat and Sentinel-2 (HLS).

3.1. WISE Algorithm

The WISE algorithm was developed and validated using VENμS Vegetation Index (VI) time-series collected over the Beltsville Agricultural Research Center (BARC) [16]. The WISE approach first uses a local moving Savitzky-Golay (SG) filter to identify spikes (e.g., undetected clouds or cloud shadows) in the NDVI time series. Observations with fitting errors larger than a predefined threshold (default: 3 standard deviations of total errors) are excluded from temporal gap-filling and smoothing. The moving window size determines the date range of samples used for smoothing and fitting. Traditionally, the SG filter uses all samples within the moving window, which works well for evenly distributed samples. However, remote sensing observations usually are not evenly distributed due to clouds or cloud shadows. To preserve local variations while filling large gaps, a flexible strategy was implemented using a maximum moving window size and a minimum number of samples. The strategy starts at the central (target) date and expands the searching dates incrementally by one day before and after. If the number of samples within the moving window reaches the minimum required number of samples, a fitting to the polynomial function will be activated to compute the value for the target date. Otherwise, the searching process continues until the moving window size reaches the defined maximum window size. If the searching reaches the maximum window size and the number of valid observations is still less than the required minimum number of samples, the algorithm stops and uses a fill value for the target date. Under the flexible strategy, periods with dense observations will use a smaller moving window, while periods with sparse observations will employ a larger moving window size. This will ensure the ability to fill large temporal gaps while still retaining variations from temporally dense observations reflected in the raw time series. Since clear HLS observations (3–4 days revisit) in the Corn Belt states are less frequent than the VENμS time series (2 days revisit) over BARC, we adjusted the required number of samples to 4 (5 in the original WISE algorithm). The maximum window size was limited to 45 days to ensure data quality (60 days in the original WISE algorithm [16]). This means that we need at least four clear observations within 90 days (±45 days) to fill a temporal gap. The new parameter setting allowed producing daily time series for most pixels in five Corn Belt states.

Once the daily VI time series is generated, the WISE algorithm uses the MACD approach to detect changing trends and then refines green-up dates using the VI time series. The MACD is computed using the differences of two exponential moving averages from short-term and long-term windows [42]:

$$MACD(t) = EMA(v(t), a) - EMA(v(t), b), \tag{1}$$

where $v(t)$ represents the daily VI time series. EMA is the exponential moving average. Parameters "a" and "b" are the moving window sizes. The resulting $MACD(t)$ is also a time series, and the change of sign from negative MACD to positive usually corresponds to an upward trend. The MACD can be used as a criterion to detect the green-up date by satisfying the following conditions:

$$MACD(t-1) < MACD\_threshold$$

and

$$MACD(t) > MACD\_threshold \tag{2}$$

where MACD_threshold is a predefined threshold for MACD (default 0 in the WISE algorithm). This is also the first internal criterion for green-up detection in the WISE algorithm. The transition date that satisfies the above condition is a solid yet delayed signal for an increasing trend [42]. We store the MACD transition date and hereafter in this paper call it the green-up date from the MACD method.

Since MACD is a delayed indicator, the green-up date from WISE algorithm is further refined using the MACD divergence (MACD_div), which is an earlier signal of change than is MACD itself. The MACD_div is computed using:

$$MACD\_div(t) = MACD(t) - EMA(MACD(t), c) \tag{3}$$

where "c" is the third window size used to compute the EMA of MACD time series. We used the same window size for a, b and c (5, 10 and 5 respectively) as examined in the original WISE algorithm. To find a transition date in the MACD time series, MACD_div need to satisfy the following conditions:

$$MACD\_div(t-1) < MACD\_div\_threshold$$

and

$$MACD\_div(t) > MACD\_div\_threshold \tag{4}$$

where MACD_div_threshold is a predefined threshold (default 0 in the WISE algorithm). This is the second criterion for the WISE algorithm. When implementing the WISE algorithm, we first use the MACD_threshold to confirm an increasing trend (Equation (2)) and then search backward to find the transition point using the MACD_div_threshold (Equation (4)). In addition to the criteria of MACD and MACD_div, the WISE algorithm requires that the green-up date must show an increase of VI than previous days over a 7-day simple moving average in the time series. Details of the WISE algorithm can be found in the original WISE paper [16].

The WISE algorithm is a near-real-time approach and can detect increasing trends in VI at a very early stage. Since some of these increasing trends are small and may not be related to crop emergence, in order to characterize the strength of a green-up event, a green-up "momentum" is also computed. The green-up momentum (or strength) is an integral of positive MACD after the green-up date divided by the number of days since green-up. A minimum green-up momentum is required to confirm a significant green-up event. In this study, we used the same threshold (0.01) to identify a substantial green-up event as in the original WISE paper.

Figure 3 shows the data flow, key parameters, and thresholds for the WISE algorithm. As described above, three main changes (maximum moving window size, minimum

number of samples, and MACD_threshold) are highlighted in red. Green-up dates from both the MACD method and the WISE algorithm are saved and evaluated.
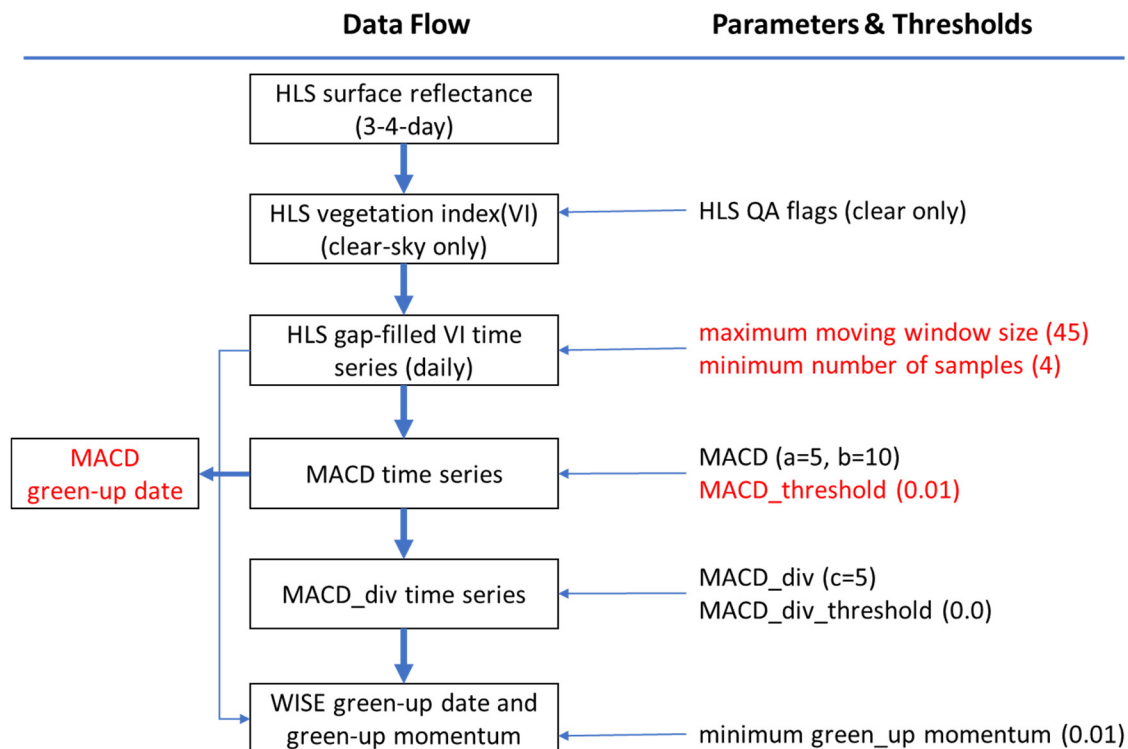

Figure 3. Data flow chart for the WISE algorithm and the MACD method. Key parameters and thresholds are listed on the right. The black text shows no change of parameter values. The red text indicates a new threshold or data compared to the original WISE algorithm.

3.2. Parameter Adjustment for Corn Belt

The MACD and MACD_div thresholds were previously trained over BARC (~150 km^2 in Maryland) using the VENμS time series. In this study, we expand the study area to ~815,500 km^2 covering the 5 primary Corn Belt states and use the HLS time series. The different ecosystems and satellite data sources involved in these two studies result in VI time series with differing characteristics, and this leads to the need for parameter refinement. The BARC fields used in the previous study [16] are usually covered by grasses/weeds/cover crops before the row crops are planted. These experimental fields in BARC are usually planted late, and soil temperature is not a controlling factor in crop emergence. Figure 4a shows a typical field in BARC that started with a low-amplitude VI cycle from the growth of weeds, followed by a strong seasonal cycle of summer crops. However, commercial farms in the Corn Belt are often planted as early as middle April [43] when the soil temperature is still low. Crops grow slowly in the early spring. Weed covers are usually treated before planting. Figure 4b shows a typical case (arsbrooks10 site in Iowa from 2020, see Table 2) in the Corn Belt that started with a flat VI curve before crop emergence and a slow increase of VI after crop emergence. The MACD curve is also flat prior to emergence. The green-up signal in the VI time series is not as marked as that in BARC. The MACD time series never have a transition date from negative to positive, and thus green-up dates might not be detected using the same thresholds from the VENμS time series in BARC. To assess MACD and MACD_div thresholds, we extracted MACD and MACD_div values for the emergence dates from 34 PhenoCam site-years and determined thresholds for MACD and MACD_div using the HLS time series in Corn Belt. The refined thresholds need to be applicable to both cases in Figure 4. We then applied the WISE algorithm to the Corn Belt states using the refined thresholds.
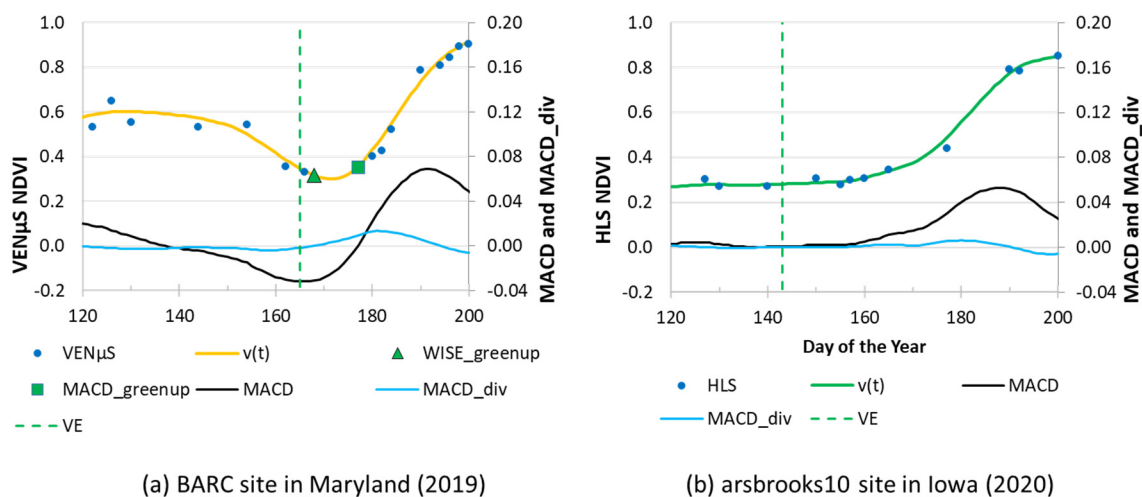
(a) BARC site in Maryland (2019)   (b) arsbrooks10 site in Iowa (2020)

Figure 4. A corn field in Maryland (**a**) and a soybean site in Iowa (**b**) show different VI time-series features. The changes of MACD and MACD_div in the BARC site (**a**) from the VENμS NDVI time series (v(t)) are more evident than those at the Iowa site (**b**) from the HLS NDVI time series. The green-up dates were not detected from (**b**) using the same thresholds used at the Maryland site (**a**). The vertical green dashed lines represent crop emergence (VE) dates derived from in situ observation.

3.3. Assessment

We first assessed green-up dates retrieved from the HLS time series over PhenoCam sites. The green-up dates from the MACD method and the WISE algorithm were compared to the observed emergence dates collected by direct visual scouting or identified from PhenoCam photos, and relevant thresholds were refined.

Using the refined thresholds, we applied the WISE approach to HLS NDVI data from 2018 to 2020 over five Corn Belt states and generated 30-m green-up maps for each year. For Iowa, where we have access to crop progress reports at sub-state scales, the maps of green-up dates were summarized at the county- and district-level for corn and soybean. At the county level, the median values of green-up dates for corn and soybeans for each county in Iowa were compared to the report planting dates from 2018–2020. At the district level, the median green-up dates for corn and soybeans were compared to the median emergence dates from the NASS Crop Progress reports for nine agricultural districts in Iowa from 2018 to 2020.

For all five states, cumulative histograms of green-up dates for corn and soybeans were computed at the state level for each year, with the pixels of each crop species derived from that year's CDL. The cumulative histograms were compared to the corresponding NASS Crop Progress reports for five Corn Belt states from 2018–2020. Statistics for PhenoCam sites and state-level comparisons include mean difference (MD), mean absolute difference (MAD), root mean squared error (RMSE), and coefficient of determination (R2). These statistics were computed for 34 PhenoCam site-years and 15 summaries at the state level (5 states by 3 years), respectively.

4. Results

4.1. WISE Parameter Adjustment

MACD and MACD_div were computed from the HLS time series for 34 PhenoCam site-years. Based on the observed or estimated emergence dates, MACD and MACD_div values on the emergence dates were extracted (Figure 5). In the scatter plot, MACD for all emergence dates are below 0.02, with most below 0.01. Since MACD is a delayed indicator for trend detection, to reduce the delay effect, we need to define a relatively small threshold that can still reliably confirm the increasing trend. In the original WISE algorithm, we adopted the typical thresholds of 0.0 for both MACD (Equation (2)) and MACD_div (Equation (4)) based on usage in stock market analyses. Considering variations in the HLS

VI time series and the frequency of clear observations in the Corn Belt, in this study, we refined the MACD threshold to 0.01. A larger MACD threshold ensures the first WISE condition can be satisfied (Equation (2)). The WISE algorithm then searches backward to find the green-up date once the MACD threshold is met (i.e., a confirmed increasing trend). We keep zero as the threshold for the MACD_div (Equation (4)) because Figure 5 shows zero is around the middle point for MACD_div, i.e., half of the green-up dates are earlier than the observed crop emergence dates, and the other half are later.
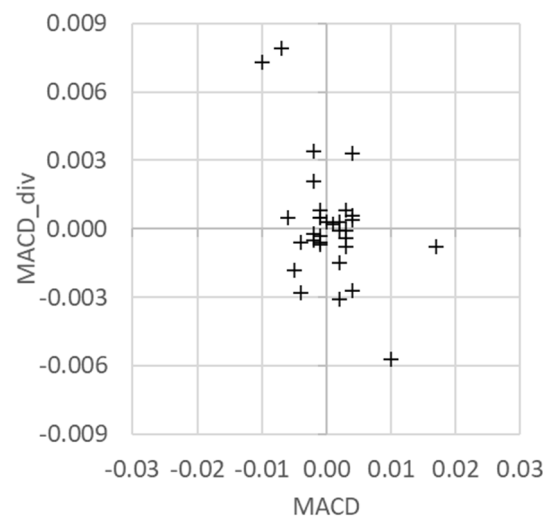
Figure 5. Scatter plot of MACD and MACD_div from the HLS time series on crop emergence dates over the 34 PhenoCam site-years. The MACD and MACD_div values determine the green-up event in Equations (2) and (4). This scatter plot can be used to determine thresholds of MACD and MACD_div for crop green-up dates over five Corn Belt states.

4.2. Green-Up Dates at PhenoCam Sites

PhenoCam site-years were used to tune the thresholds of MACD (Equation (2)) and MACD_div (Equation (4)) in the WISE algorithm. Green-up dates from the MACD method and the WISE algorithm were compared to crop emergence dates to assess the relative performance of the two approaches. Figure 6 shows scatter plots between crop emergence dates and green-up dates from the WISE algorithm (Figure 6a) and the MACD method (Figure 6b). Again, the MACD method is based only on criterion 1 (Equation (2)), while in WISE both criteria 1 and 2 (Equations (2) and (4)) are enforced. Most green-up dates from WISE are close to crop emergence dates (e.g., C1 and S1) along the 1:1 line in Figure 6a. However, some sites (e.g., C2 and S2) were estimated late, while others (e.g., C3 and C4) were estimated early. We will examine those sites later.

For the MACD method using the MACD_threshold of 0.01, green-up dates were all later than emergence dates (Figure 6b), which confirms that MACD is a delayed indicator for green-up detection. Table 3 shows the statistics between emergence dates and green-up dates from the WISE algorithm and the MACD method. The WISE algorithm produced green-up dates on average 3 days later than emergence dates, while the MACD method detected green-up (MACD transition) dates 14 days later. The results from the WISE algorithm agreed with the original findings from the VENμS time series over BARC (4–5 days after emergence). The green-up dates from the MACD method are close to the curvature-based approach that produced the green-up dates about 2–3 weeks after crop emergence [13,17]. The R-square for the MACD method (0.79) is slightly higher than the WISE algorithm (0.72), suggesting that MACD is still a solid indicator for crop emergence even though it is a delayed indicator.
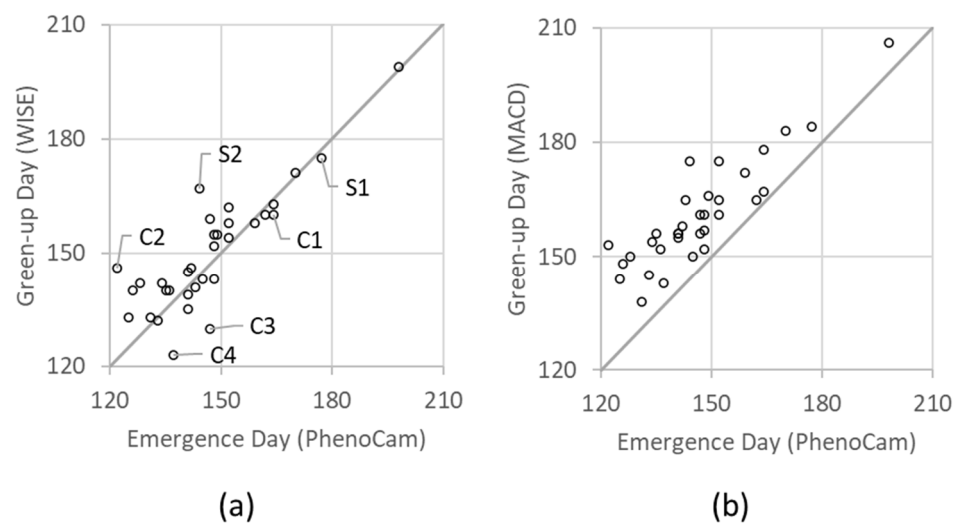
Figure 6. Scatter plots between crop emergence dates (day of the year) and green-up dates from the WISE algorithm (**a**) and the MACD method (**b**) for PhenoCam site-years. Selected points, indicated by labels ("C" for corn and "S" for soybean), demonstrate close (C1 and S1), late (C2 and S2), and early (C3 and C4) detections from WISE. These sites are further analyzed in Figure 7. Green-up dates from the MACD method (**b**) were all detected late.
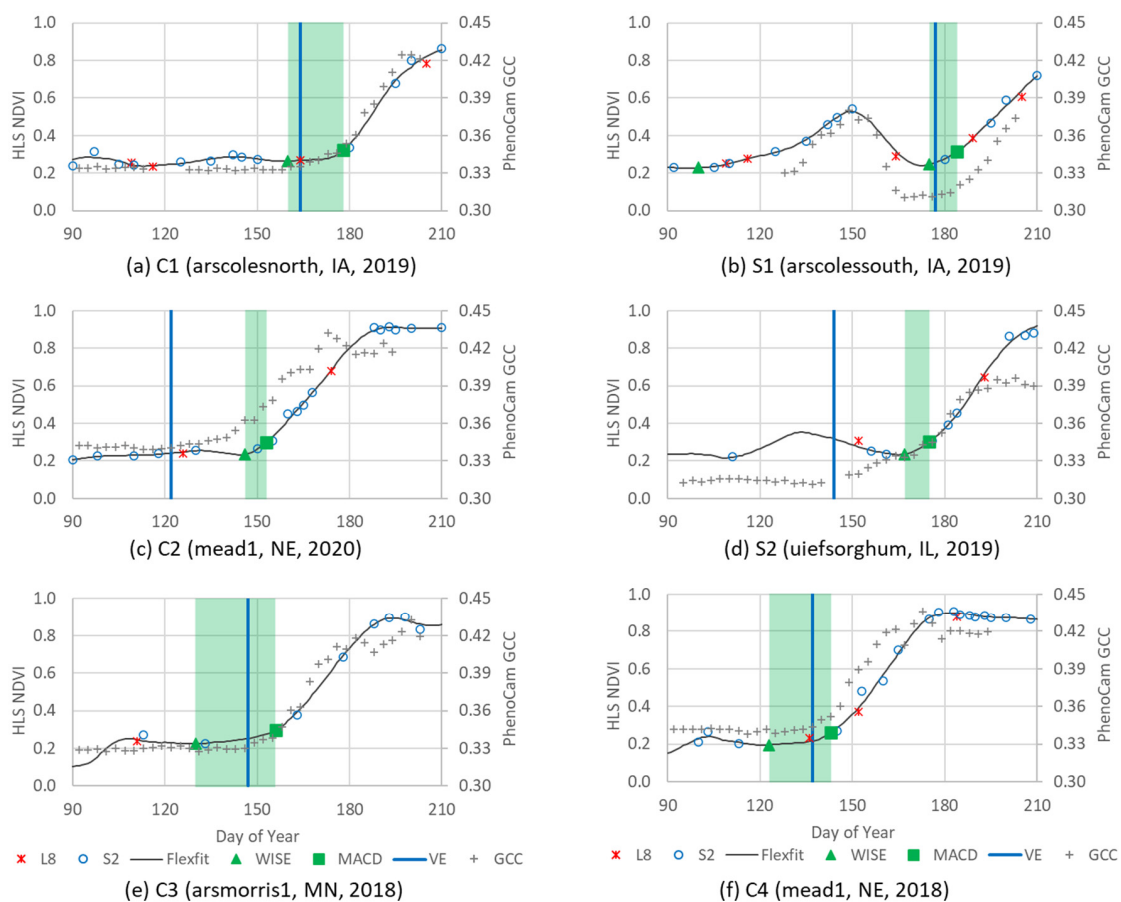

Figure 7. Landsat 8 (L8), Sentinel-2 (S2), the fitted NDVI time series (Flexfit), remote sensing green-up dates (WISE and MACD), PhenoCam GCC time series (GCC), and ground observed or photo-interpreted crop emergence (VE, blue vertical line) for the six selected sites (labeled in Figure 6). The light green area shows the period of two green-up dates detected using the WISE algorithm and the MACD method. The selected examples show close (**a,b**), late (**c,d**), and early (**e,f**) detections of crop emergence using the WISE algorithm for corresponding HLS 30-m pixel.

Table 3. Statistics between crop emergence and green-up dates detected from the HLS time series using the WISE algorithm and the MACD method over PhenoCam sites.

Statistical Metrics	WISE	MACD
Mean Difference (MD, days)	3.0	14.1
Mean Absolute Difference (MAD, days)	6.6	14.1
Root Mean Square Error (RMSE, days)	9.0	15.8
Coefficient of determination (R^2)	0.72	0.79

To further investigate the performance of WISE algorithm, we selected four corn sites ("C") and two soybean sites ("S") labeled in Figure 6a to examine in detail. Figure 7 shows Landsat and Sentinel-2 observations, NDVI time series, green-up dates from the WISE algorithm and the MACD method, and crop emergence dates for each of these six representative sites (also underlined in Table 2). Among the six selected sites, the corn site "C1" (Figure 7a) and soybean site "S1" (Figure 7b) show reasonable estimations of crop emergence from WISE. In Figure 7a, time series patterns from HLS NDVI and PhenoCam GCC were similar even though they have different absolute values. The WISE algorithm captured the green-up date that was closer to the crop emergence date compared to the MACD method. In Figure 7b, there was a slight increase of NDVI and GCC around day 150 (30 May 2019) due to the cover crop, similar to typical cases in BARC (Figure 4a), while soybean emerged on day 177 (26 June 2019). The WISE algorithm used the full time series up to day 228 (16 August 2019) and captured green-up events for the cover crop on day 100 (10 April 2019) and soybean on day 175 (24 June 2019). Soybeans showed more substantial green-up momentum (0.026) than did the cover crop (0.012), and thus, the later and stronger green-up event from soybeans was chosen in the final output, although both pieces of information may be useful for some applications. This case is similar to the BARC experimental fields in Maryland. The WISE algorithm can capture all substantial green-up events (i.e., green-up momentum > 0.01), an essential feature for double crops or crops with multiple growth cycles such as alfalfa. Please note that if we run WISE using time series only up through July (e.g., day 182), we might not confirm the green-up event for soybeans due to a small green-up momentum.

Green-up dates at corn site "C2" and soybean site "S2" were detected later than emergence dates (Figures 6a and 7c,d). At site "C2" (mead1 site in Nebraska from 2020), corn emerged on day 122 (1 May 2020), while the green-up event was detected on day 146 (25 May 2020) (Figure 7c). The HLS NDVI time series was flat before day 130 (Sentinel-2 NDVI = 0.256). The following clear observation was acquired on day 150 (Sentinel-2 NDVI = 0.265 or an increase of 0.009 in 20 days) and was then followed by a substantial increase of NDVI on day 153 (Sentinel-2, NDVI = 0.295 or an increase of 0.03 in 3 days) and day 155 (Sentinel-2, NDVI = 0.309 or an increase of 0.014 in 2 days). The WISE algorithm estimated a substantial green-up date on day 146 (25 May 2020), which was still reasonable based on available HLS observations. However, the GCC time series from PhenoCam showed a stronger green-up signal earlier than HLS, which suggests that the crops over the 30-m pixel area might not have emerged uniformly or that the field of the view from PhenoCam was different from the HLS pixel. Microclimate and other within-field factors may cause different timings of crop emergence within the field. The site "S2" (uiefsorghum in Illinois) was planted with soybean in 2019 that emerged on day 144 (24 May 2019) (Figure 7d). From day 112 to 151, there was a 40-day gap without any clear Landsat or Sentinel-2 observation. The SG filter filled the gap using four observations before and after the gap period and had a small peak of NDVI around day 135 and then an increasing trend from day 161 (NDVI = 0.237) to day 176 (NDVI = 0.309) from Sentinel-2 observations. Based on the second (stronger green-up momentum) increasing trend, WISE detected the green-up event on day 167 (16 June 2019). However, the PhenoCam GCC time series did not show the small peak around day 135. The HLS time series was affected by three available observations (days 152, 156, and 161) after day 135, which showed a de-

creasing trend of NDVI and caused the small peak in the gap-filling. The discrepancy may be due to the different fields of view or noise from HLS data (day 156 was a cloudy day).

Two corn sites (C3 and C4) detected green-up dates that were earlier than crop emergence dates. Both sites show a gradual increase of NDVI during the period of emergence. Figure 7e (arsmorris1 in Minnesota from 2018) shows emergence on day 147 (27 May 2018) from PhenoCam photos. However, from day 121 (1 May 2018) to day 181 (1 July 2018), there were only three clear observations on days 133, 163, and 178 from Sentinel-2 in 60 days. The WISE algorithm estimated the green-up date on day 130 (10 May 2018). The MACD method detected green-up at a much later date (day 156 or 5 June 2018). The emergence date was between the two green-up dates detected from WISE and MACD. Figure 7f (mead1 in Nebraska from 2018) shows a similar result in Figure 7e. The field-observed emergence date (day 137) was between the green-up dates detected by WISE (day 123) and MACD (day 143). The Mead site in Figure 7f had 8 clear Landsat-8 and Sentinel-2 observations from day 121 to 181, which were very frequent and captured corn growth well. The uncertainty of green-up detection for site C4 was mainly due to the flat VI time-series in the early growing stage, which is a challenge for phenology mapping approaches.

4.3. Assessment at County and District Level in Iowa

Green-up dates derived with WISE-HLS for corn and soybean were summarized and compared to the planting dates for each county in Iowa from 2018 to 2020, using the CDL from each year as the crop mask. Figure 8 shows scatter plots between the median green-up dates from HLS and the planting dates from NASS for each county in Iowa and for each year. As expected, median WISE green-up dates at the county level were generally after the planting dates. The relationships between planting dates and green-up dates vary by year and county. The median days from planting to green-up for corn were about 12, 22, and 26 days from 2018–2020, while soybeans took slightly less time (11, 15, and 22 from 2018–2020) from planting to green-up. The days from planting to emergence reported by NASS for Iowa were 9–19 days, less than the days from planting to the WISE green-up dates. This implies that the WISE green-up dates are slightly later than emergence dates, which agrees with the results from PhenoCam sites.
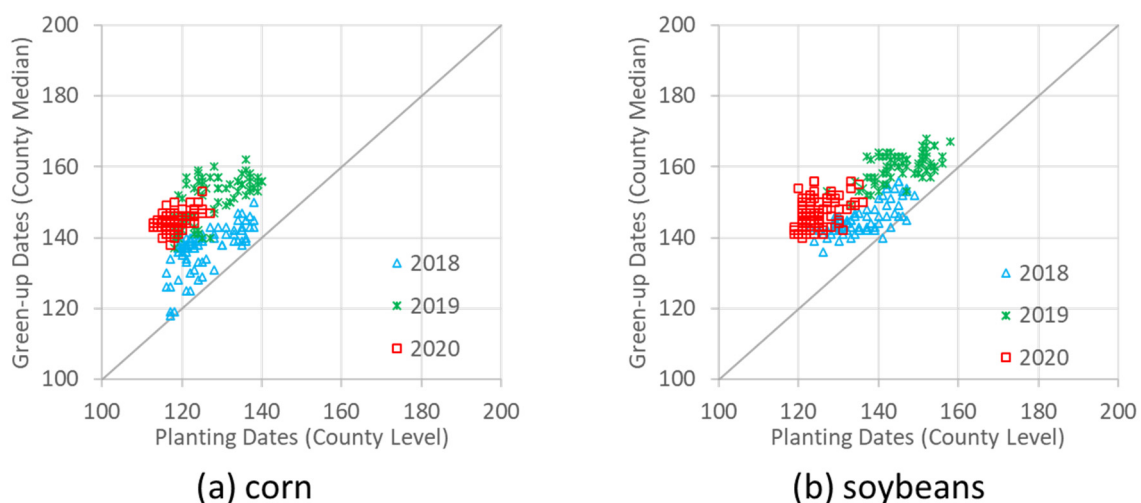

Figure 8. Scatter plots of average planting dates from NASS and median green-up dates from HLS time series for corn (**a**) and soybeans (**b**) from 2018–2020. Each symbol represents a county-year in Iowa.

Among the three years, the difference between planting and green-up dates was the smallest in 2018. Green-up dates for some counties were close to or even a few days earlier than planting dates in 2018. This may be due to several reasons. First, the samples used in producing county-level planting (field survey) and green-up dates (HLS images) are different from different years. Second, differences in soil temperature and moisture could

lead to a time difference from planting to emergence. In 2018, the accumulated growing degree days in May were above the climatology while 2019 and 2020 were under [44], which could lead to a more rapid emergence in 2018. Since soybeans were planted late in 2019 (from middle May to early June), the temperature was high, and it took less time from planting to green-up. Third, the difference in frequency of clear-sky images could be another cause of variation. In comparison, percentages of clear observations per day in Iowa in May were 9.4% in 2018, 8.6% in 2019, but 6.5% in 2020.

We also compared crop emergence and green-up dates at the district scale for nine agricultural districts in Iowa, each of which contains multiple counties. Figure 9 shows scatter plots between median emergence dates from the NASS crop progress reports and median green-up dates summarized from 30-m HLS pixels for each district. Generally, green-up dates from WISE-HLS captured the variability of emergence dates at the district level. There were some early estimations for soybean in 2018 and 2019 and late estimations for corn in 2020 compared to emergence dates at the district level. The mean differences between median green-up and emergence dates from nine districts were −1 to 8 days for corn and −4 to 1 days for soybeans in three years. The R^2 was 0.74 based on 54 points (9 districts, 3 years, and 2 crops). In 2020, the WISE green-up dates for corn were similar across districts, which may be due to the low frequency of clear-sky imagery in the year (6.5% clear observations per day in May).
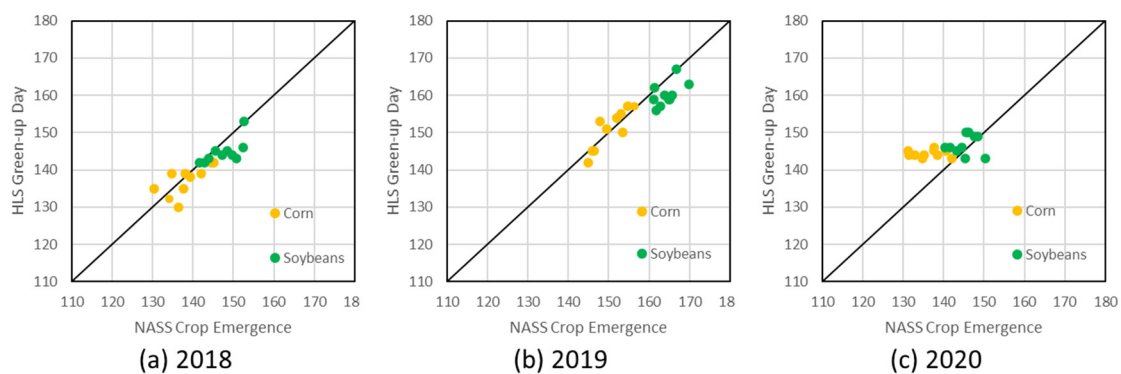

Figure 9. Scatter plots between the median crop emergence dates from crop progress reports and median green-up dates from HLS for 2018 (**a**), 2019 (**b**), and 2020 (**c**). Each point represents an agricultural district for corn (yellow) or soybean (green).

4.4. Assessment at State Level

Finally, green-up dates from the WISE algorithm for five Corn Belt states were summarized at the state level and compared to the crop emergence dates reported by NASS for each state. Figure 10 shows the cumulative percentage histogram of emergence dates from NASS (dashed line) and green-up dates from the WISE algorithm (solid line) using HLS. The cumulative histograms for emergence dates and HLS green-up dates are similar and vary by year and state. Figure 10 shows that crop emergence dates were earlier in 2018 and later in 2019 for all five Corn Belt states, while in 2020, relative emergence varied by state. For example, crop emergence dates in 2020 (red dashed line) were close to 2018 in Iowa, Minnesota, and Nebraska (Figure 10a,b,g–j) and were between 2018 and 2019 in Illinois and Indiana (Figure 10c–f). The differences in corn and soybean emergence dates for different states ranged from 1 to 4 weeks between 2018 and 2019. Generally, the HLS green-up dates (yyyy_RS) captured annual variations and agreed with the reported crop emergence dates (yyyy_VE). For most years and states, the green-up dates were slightly later than emergence dates. A few state-year instances show green-up dates were somewhat earlier (e.g., Indiana-2018 and Minnesota-2018). From 2018 to 2020, crop emergence dates and HLS green-up dates for Illinois and Indiana were more diverse, with larger inter-annual differences in Figure 10c–f, than for the other three states.
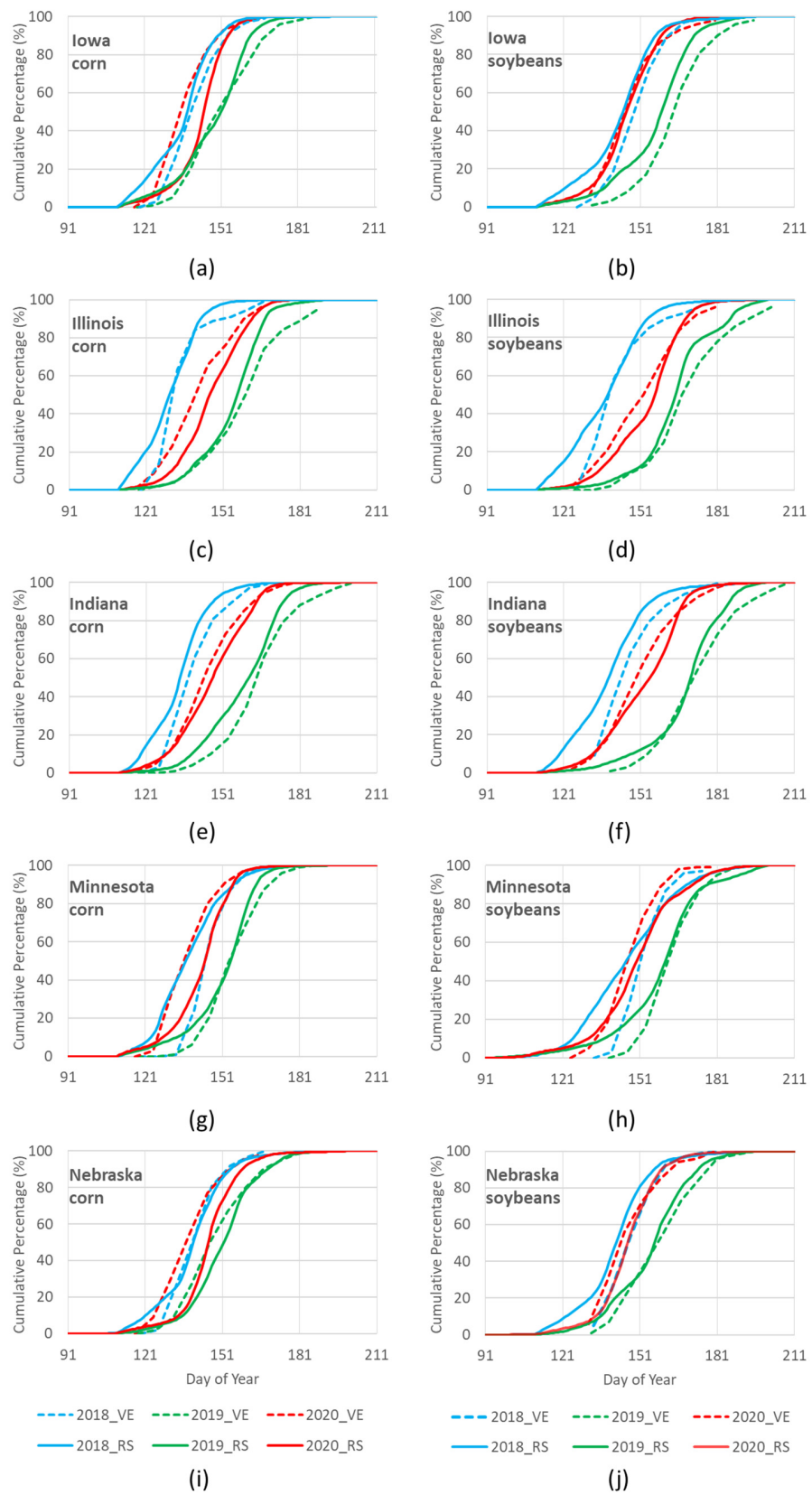
Figure 10. Cumulative histograms of crop emergence (VE, dashed lines) from NASS crop progress reports and green-up dates from remote sensing (RS, solid lines) for corn left panel, (**a,c,e,g,i**) and soybeans (right panel, **b,d,f,h,j**) over Iowa (**a,b**), Illinois (**c,d**), Indiana (**e,f**), Minnesota (**g,h**), and Nebraska (**i,j**) from 2018 to 2020.

To assess the agreement between green-up and emergence dates quantitatively, median dates of green-up and emergence in Figure 10 were extracted for each state and year, yielding 15 points in total, and were compared in Figure 11. The median green-up dates agree with the median emergence dates. For example, the WISE-HLS green-up dates capture the late emergence in 2019 and the earlier emergence in 2018.
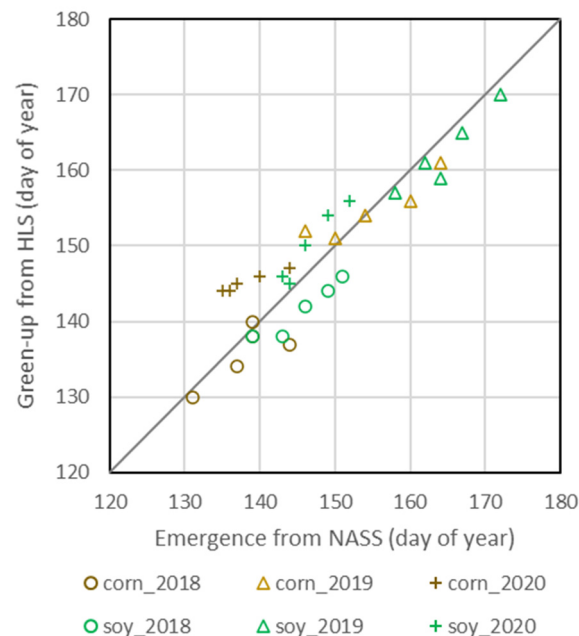
Figure 11. Scatter plot of median emergence dates from NASS crop progress reports and median green-up dates retrieved from HLS time series for five states from 2018–2020.

Table 4 provides a listing of differences between remote sensing median green-up and reported median emergence dates, as well as statistical metrics of agreement. Based on these 15 data points, the average differences were 1.5 days for corn and −0.9 days for soybeans. The mean absolute differences were 3–4 days, and the root mean square errors were 3–5 days. The range of disagreement was between −7 to 9 days for corn and −5 to 5 days for soybeans. In general, remotely sensed green-up dates for soybeans were closer to emergence dates than for corn. The detected green-up dates in 2020 were later than the reported emergence dates, especially for corn in Iowa (9 days), Minnesota (8 days), and Nebraska (8 days). However, the detected green-up dates were close to emergence dates in 2018 and 2019 for those three states, and crop emergence dates in 2018 and 2020 were close. This implies that the delayed detection may be due to the availability of clear remote sensing observations in the 2020 emergence period.

Table 4. Statistics of differences (the number of days) between HLS green-up dates and NASS emergence dates for five states from 2018 to 2020.

Year	State	Corn	Soybeans
2018	Iowa	−1	−5
	Illinois	−1	−1
	Indiana	−3	−5
	Minnesota	−7	−5
	Nebraska	1	−4
2019	Iowa	1	−5
	Illinois	−4	−2
	Indiana	−3	−2
	Minnesota	0	−1
	Nebraska	6	−1
2020	Iowa	9	1
	Illinois	6	4
	Indiana	3	5
	Minnesota	8	4
	Nebraska	8	3
Mean Difference (MD, days)		1.5	−0.9
Mean Absolute Difference (MAD, days)		3.9	3.1
Root Mean Square Error (RMSE, days)		5.0	3.6
Coefficient of determination (R2)		0.73	0.87

4.5. Green-Up Mapping

Using time-series HLS data from January 1 (day 1) to middle August (day 228) each year, we generated maps of WISE-derived green-up dates at 30-m resolution from 2018–2020. Figure 12 shows the mosaicked map of the 2019 green-up dates (a) and CDL (b) for five Corn Belt states (maps for 2018 and 2020 see Appendix A Figures A1 and A2). The delay in planting in 2019 over the Corn Belt varied by state. Median emergence dates for corn and soybean in Illinois and Indiana were delayed for about 4 weeks, while median emergence dates in Nebraska were only delayed 1–2 weeks [7] compared to 2018. This led to an even higher spatial variability of crop emergence dates in 2019. Figure 12 shows that natural vegetation (e.g., northeast of Minnesota and west of Nebraska) greens up earlier than croplands. Illinois and Indiana had later green-ups (days 156–161 for corn, and 165–170 for soybeans) than the other three states (152–154 for corn and 157–161 for soybean) in 2019. However, Illinois and Indiana were the two states that showed earlier green-up dates (days 130–134 for corn and day 138 for soybeans) than the other three states (137–140 for corn and 142–144 for soybeans) in 2018. Figure 12 captures the spatial variability of green-up dates for different states and provides great spatial details within states, districts, counties, and fields. Artifacts related to clear-sky image availability are also apparent in this map. The streak across Iowa highlights a higher density of pixels for which green-up dates could not be detected, due to a paucity of clear Landsat or Sentinel-2 observations during the 2019 early growing season. The northeast–southwest streak boundaries are along the Sentinel-2 swath boundaries. The streak area had fewer Sentinel-2 observations (no overlap) and was cloudy during the early growing season. Even using the 3–4-day revisit HLS data, green-ups for some regions still cannot be detected, which highlights the need for high-frequency imaging.
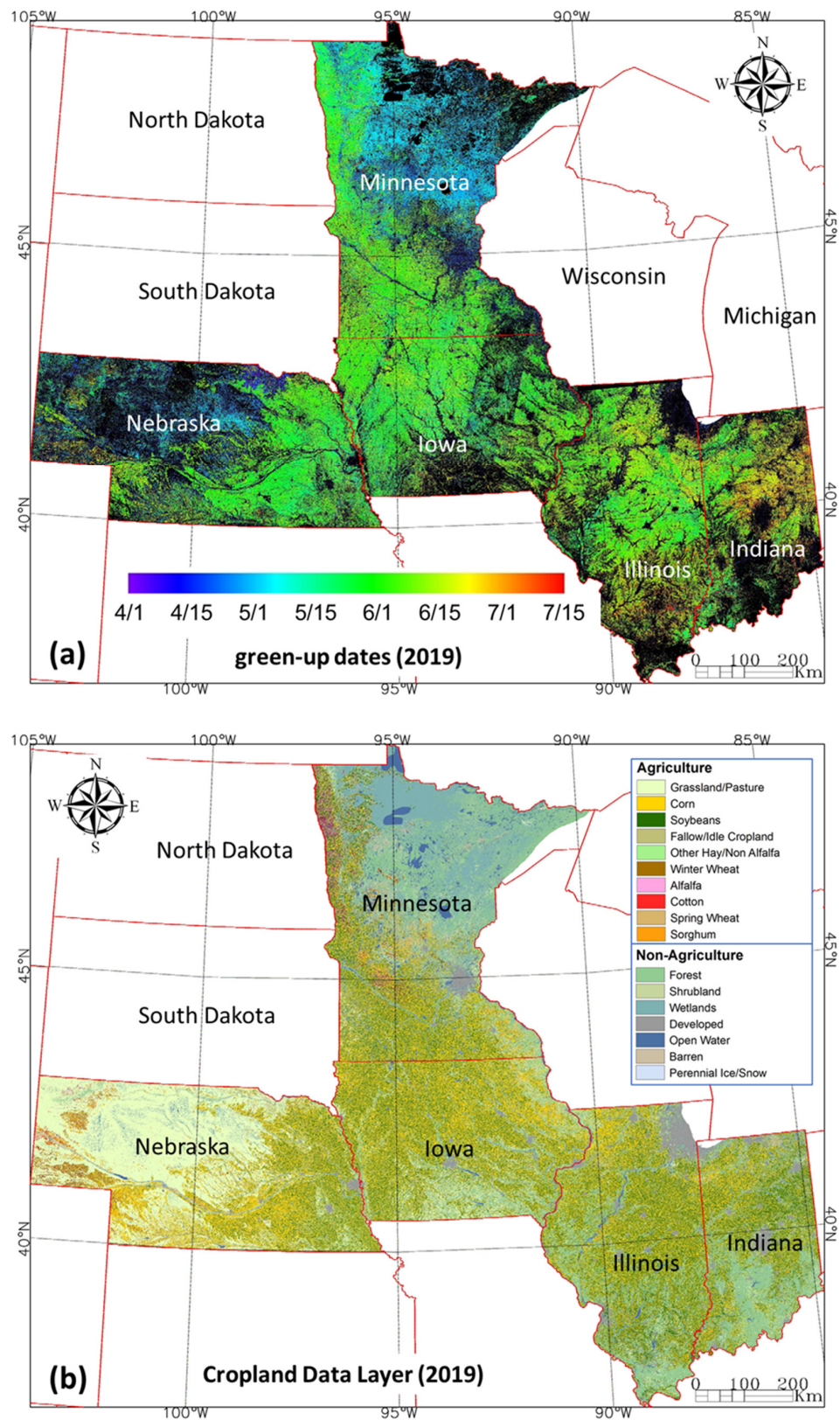
Figure 12. Green-up dates (**a**) produced using the HLS time series from 1 January 2019 to 16 August 2019 and the 2019 Cropland Data Layer (CDL) (**b**) for five Corn Belt states (Albers equal-area projection). Different colors in (**a**) represent different green-up dates (month/day under the color bar). Black color indicates that green-up dates cannot be detected.

According to the NASS crop progress reports, among these five states, Illinois had the highest degree of inter-annual variability in crop emergence. In agreement with reported emergence dates, the WISE green-up dates over Illinois were earliest in 2018 and latest in 2019, particularly in northern Illinois (Figure 13). This was related to historical cool and wet weather in 2019. Some fields were not planted at all. According to the USDA Farm Service Agency (FSA) crop acreage report [45], Illinois has the largest amount of prevented planting areas among five states in 2019.
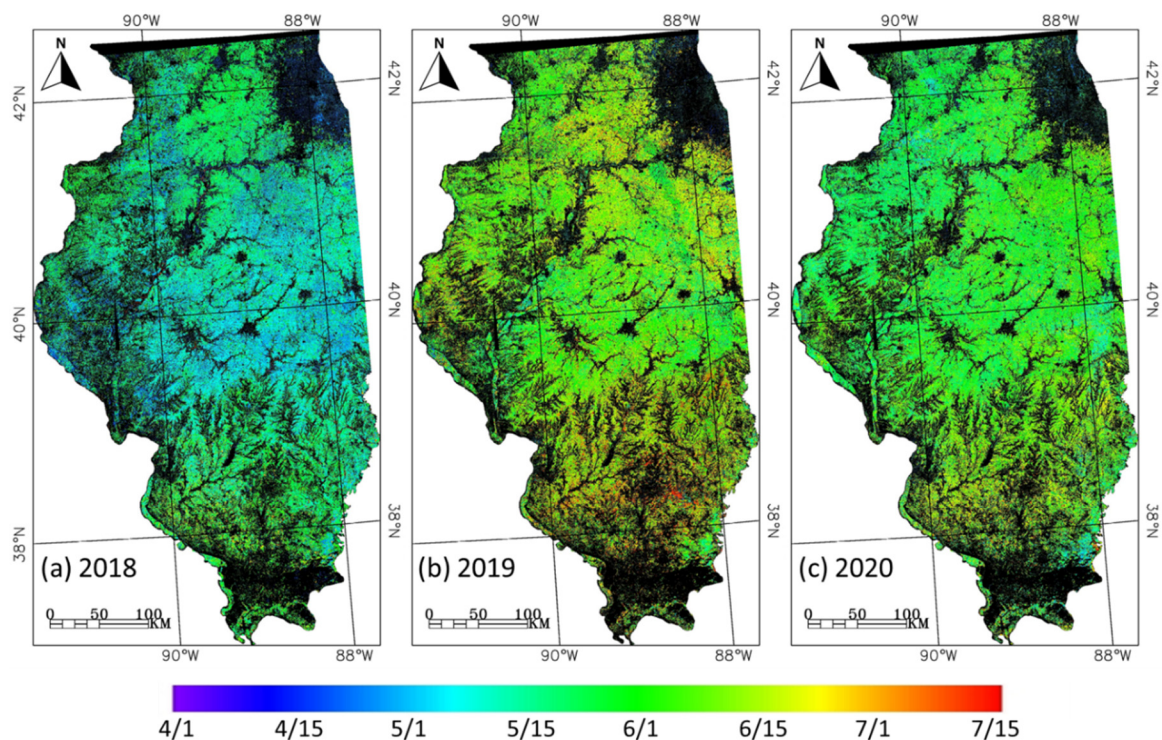
Figure 13. Green-up dates for Illinois from 2018 to 2020. (**a**–**c**) Crops emerged earliest in 2018 and latest in 2019 (Albers equal-area projection). Black pixels show that green-up events are not substantial or lack HLS observations for detection.

5. Discussion

5.1. Algorithm Parameters

The WISE algorithm has been demonstrated effective in detecting green-up dates using the VENμS (2-day) and HLS (3–4-day) time series. As with all phenology algorithms, the green-up detection depends on the frequency of remote sensing observations and cloud conditions related to season and location. The WISE algorithm includes two sets of parameters (i.e., VI gap-filling process and green-up detection) that may need adjustments for a new data source or location. The gap-filling process is geared toward filling most temporal gaps in the VI time series while retaining local variations. In the previous study over Beltsville, Maryland [16], we used at least 5 samples within the moving window for the VENμS time series (2 days revisit). To achieve reasonable results in this study using HLS time series with lower revisit frequency (3–4 days), we reduced this to requiring 4 samples over a 90-day window. For cloudy periods, we may need an even longer moving window to fill a sizeable temporal gap. However, a large moving window may result in low-quality filling and affect the green-up detection.

Remote sensing VI time series may have distinct features in different regions relating to climate or land management. For example, in Maryland, we usually see a small peak in VI before emergence due to weeds or winter cover crops. In the Corn Belt states, most of the VI time series for crops are flat before emergence. The WISE algorithm works better when a small peak appears before emergence in the VI time series (e.g., Maryland case) since MACD is more sensitive to such change. In contrast, MACD is not very sensitive to

flat curves, which challenge all phenology mapping methods. In this paper, MACD and MACD_div thresholds were set as 0.0 and 0.01 based on PhenoCam observations in the region. They may need to be further tuned using additional local observations and remote sensing time series.

5.2. Validation and Comparison

In this paper, we refined the WISE algorithm and assessed green-up dates using crop emergence dates over 34 site-years with PhenoCams in Corn Belt. Even though we can compare green-up dates to the reported planting and emergence dates at the county, district, and state levels, sampling locations from field surveys and HLS image pixels are different. Field-scale validation data for agroecosystems actively managed year-to-year are rare and needed to improve broad-scale efforts to monitor productivity, yield, and crop phenology [31]. PhenoCams are one such data resource. Since PhenoCam data are limited by the camera field of view and photo resolution, ground observations at the field scale are also needed, especially over various agroecosystem regions.

The HLS green-up dates from the WISE algorithm show some earlier or later detections than crop emergence dates, while the MACD method always detected later than emergence dates. This agrees with the general remark that MACD is a delayed indicator for trend detection. The MACD produced green-up dates 2–3 weeks after crop emergence, which is close to the previous study in Iowa that used the entire year of Landsat and MODIS data fusion for crop phenology mapping based on VI amplitude or curvature approaches [13]. The within-season approach (WISE) produced the green-up dates earlier than after-season mapping methods [13,17].

5.3. Challenges on Near-Real-Time Mapping and Future Improvements

Near-real-time mapping of crop emergence is challenging since early detections could be affected by the availability of observations in the early growing season, the sensitivity of crop emergence in the VI time series, and remote sensing data quality. Green-up is a slight change of the VI trend in the first few days after emergence, and noise (e.g., undetected clouds and cloud shadows) may affect the ability to robustly detect green-up [12]. Therefore, a high-quality and temporally consistent time series is required in the near-real-time green-up mapping. For the WISE algorithm, the relative consistency of the VI time series is more important than the absolute accuracy of VI. For time series combining multiple sensors, preprocessing such as BRDF and bandpass correction in HLS may be needed.

This study demonstrates that the 3–4 day HLS is frequent enough for most of our study area. The current HLS dataset only includes Landsat-8 and Sentinel-2 (a and b). Landsat 9 was launched on 27 September 2021 and can further increase the frequency of the HLS dataset. The PlanetScope constellation includes over 100 CubeSats in low earth orbits [46,47]. The PlanetScope fused (L3H) data products provide spatially and spectrally consistent surface reflectances (daily, 3-m) [47], which could be used for mapping crop emergence [15,48], especially for small fields and crop management activities. The spatial-temporal data fusion approach has not been evaluated in the near-real-time mapping since data consistency and accuracy are more critical in near-real-time (within-season) mapping than after-season mapping. Although spatial-temporal data fusion can increase the frequency of high-resolution data, these fused data are subject to uncertainties and noise. The after-season approaches can use complete time series while the near-real-time approaches only use a partial year of data, and thus, the influence of signal-to-noise ratio is greater in near-real-time approaches. For green-up date mapping, spatial-temporal data fusion approaches are more useful for historical years before the Sentinel-2 era [13].

As demonstrated in our previous study, the WISE algorithm can run routinely every few days or weeks [16]. The WISE method can produce both green-up dates and green-up momentum. Green-up momentum can be used to determine the significance of a green-up event. There could be multiple green-up events from grasses and crops during the early growing season. To distinguish crop emergence from grasses in the early stage, we need

ancillary information such as the usual crop growth calendar or we may need to wait for more days to confirm. Green-up momentum for crops is usually higher than grasses and can be confirmed a few weeks after emergence.

This paper only used VI time series in green-up detection. Results may be further improved by incorporating other information such as land surface temperature, soil moisture, and usual planting/emergence dates. Land surface temperature and soil moisture at a coarse spatial resolution are available from satellite remote sensing and may be included in the future. Usual planting/emergence dates are available from NASA at the state level [43]. They can be used to filter green-up events outside the date ranges from grasses or cover crops.

The WISE algorithm can run in near real time. However, producing near-real-time phenology data products is still challenging and limited by several factors. First, the WISE algorithm requires a substantial green-up momentum (>0.01) to confirm a crop emergence event, which usually needs 1–2 weeks for crops to grow after emergence from the previous study [16]. Second, remote sensing data have latency in data acquisition and processing. This paper used the HLS surface reflectance data product, available ~6 days after Sentinel-2 or Landsat overpass dates. Third, the processing time, including data download, gap-filling, and green-up mapping, took about 1–2 days for one state in a Linux system (19 processors at 3.07 GHz each). Adding all factors together, the mapping time of crop emergence dates takes 2–3 weeks after crop emergence using the WISE approach and HLS time series. Some operational programs such as the NASS crop progress reports need to be generated and released every week during the crop growing season, which is still challenging for remote sensing approaches. Reducing the latency of satellite data products and using high-performance computing can shorten mapping time. Nevertheless, the WISE approach still needs 1–2 weeks for crops to grow large enough to be detectable and separable from other background variations such as the changes in soil conditions. Cloud contamination may further delay the detection, especially when clouds continuously occur after crop emergence.

6. Conclusions

Crop emergence is the first critical stage for crop growth monitoring. Remote sensing data are used to detect crop green-up dates relating to crop emergence dates. This paper extends a within-season emergence (WISE) algorithm for mapping crop emergence dates using the routine Harmonized Landsat and Sentinel-2 (HLS). Remotely sensed green-up dates in five Corn Belt states (Iowa, Illinois, Indiana, Minnesota, and Nebraska) were mapped from 2018 to 2020 and compared to independent observations of planting and emergence dates from PhenoCams at local scales and NASS at district and state scales. Results show that remotely sensed green-up were typically within one week of corn and soybean emergence. HLS green-up maps were able to capture the late emergence (1–4 weeks delay) of crops in 2019 in Corn Belt states, resulting from late planting due to exceptionally wet spring that year.

This study demonstrates that the operational mapping of crop emergence dates at field scale (30-m) over a large region is practicable using routine HLS data. Crop emergence mapping within the season using a partial year of time series is feasible. Further work is needed for additional validation at the field scale using ground observations, especially in different agroecosystem regions. Uncertainty of green-up dates from the WISE algorithm needs to be further assessed for different locations and years. Landsat 9 adds additional observations and will be included and evaluated for crop emergence mapping.
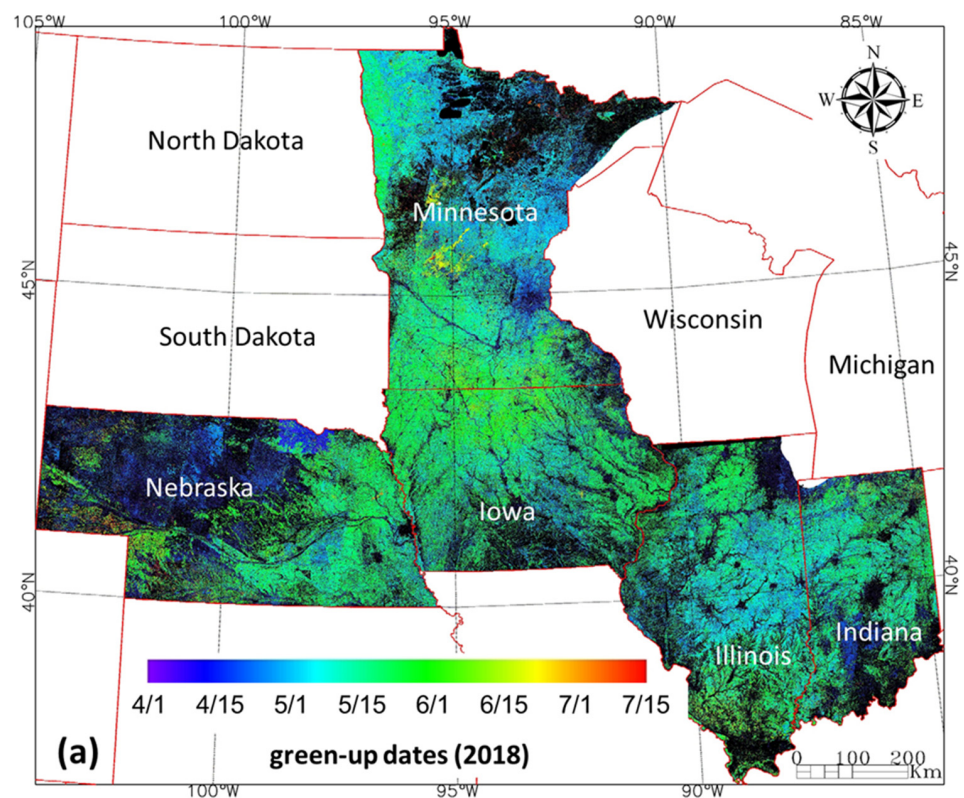
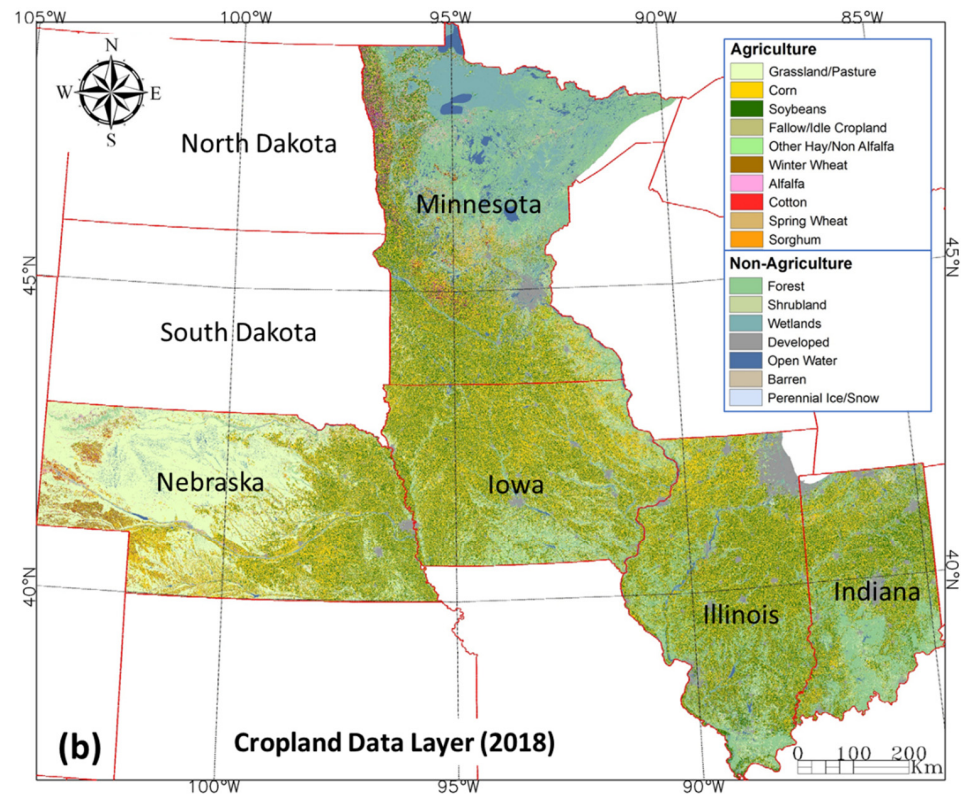## Appendix A

Figure A1. *Cont.*

Figure A1. Green-up dates (**a**) produced using the HLS time series from 1 January 2018 to 16 August 2018 and the 2018 Cropland Data Layer (CDL) (**b**) for five Corn Belt states. Black color indicates that green-up dates cannot be detected.

Figure A2. *Cont*.

Figure A2. Green-up dates (**a**) produced using the HLS time series from 1 January 2020 to 16 August 2020 and the 2020 Cropland Data Layer (CDL) (**b**) for five Corn Belt states. Black color indicates that green-up dates cannot be detected.
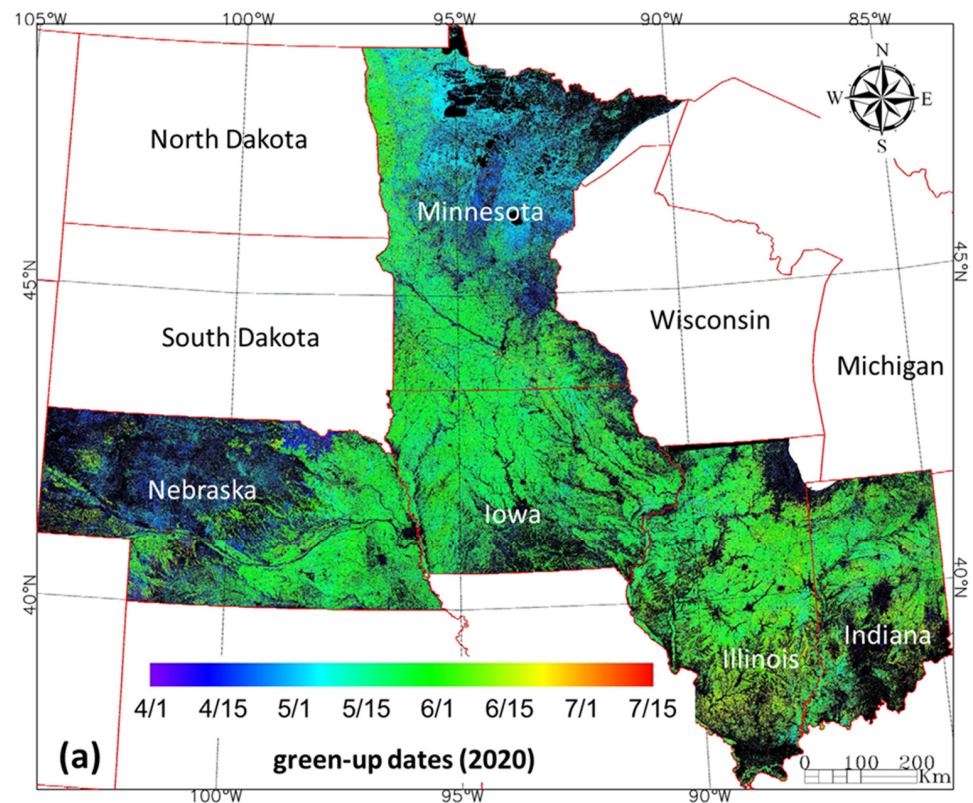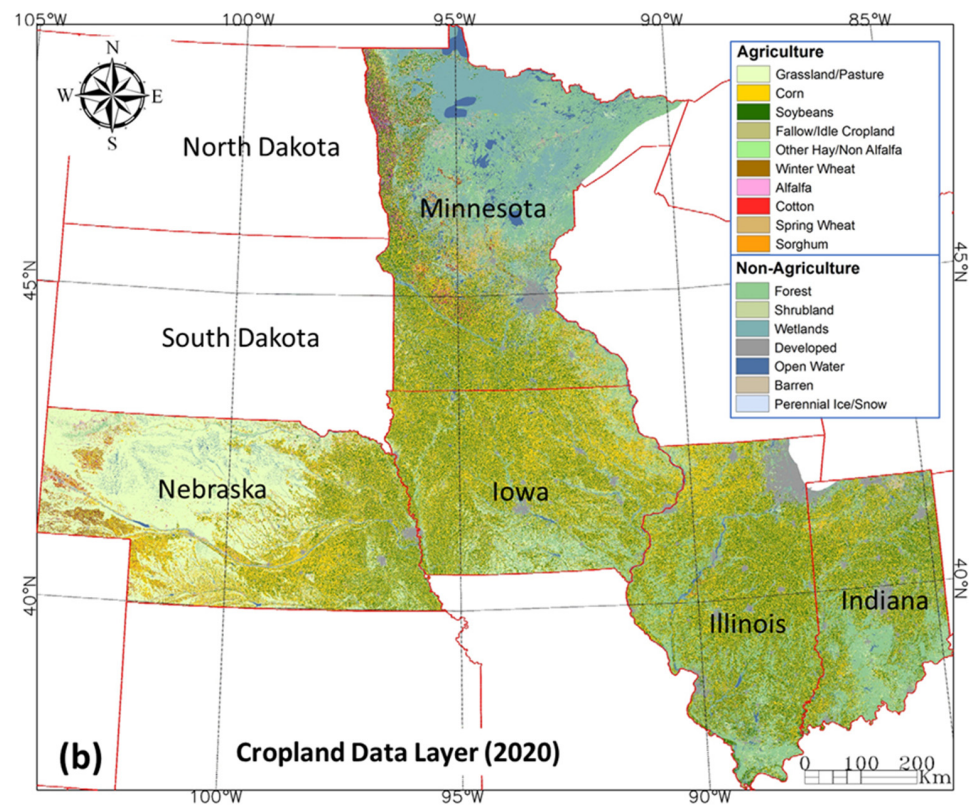
References

1. Kucharik, C.J. A Multidecadal Trend of Earlier Corn Planting in the Central USA. *Agron. J.* **2006**, *98*, 1544–1550. [CrossRef]
2. Walthall, C.L.; Hatfield, J.; Backlund, P.; Lengnick, L.; Marshall, E.; Walsh, M.; Adkins, S.; Aillery, M.; Ainsworth, E.A.; Ammann, C.; et al. *Climate Change and Agriculture in the United States: Effects and Adaptation*; USDA Technical Bulletin 1935; USDA: Washington, DC, USA, 2012; 186p.
3. Neild, R.E.; Newman, J.E. Growing Season Characteristics and Requirements in the Corn Belt. NCH-40. Cooperative Extension Service, Purdue University. Available online: https://www.extension.purdue.edu/extmedia/nch/nch-40.html (accessed on 8 November 2021).
4. Rosenzweig, C.; Jones, J.W.; Hatfield, J.L.; Ruane, A.C.; Boote, K.; Thorburn, P.; Antle, J.M.; Nelson, G.C.; Porter, C.; Janssen, S.; et al. The Agricultural Model Intercomparison and Improvement Project (AgMIP): Protocols and pilot studies. *Agric. For. Meteorol.* **2013**, *170*, 166–182. [CrossRef]
5. Yang, Y.; Anderson, M.C.; Gao, F.; Wardlow, B.; Hain, C.R.; Otkin, J.A.; Alfieri, J.; Yang, Y.; Sun, L.; Dulaney, W. Field-scale mapping of evaporative stress indicators of crop yield: An application over Mead, NE, USA. *Remote Sens. Environ.* **2018**, *210*, 387–402. [CrossRef]
6. Müller, C.; Elliott, J.; Kelly, D.; Arneth, A.; Balkovic, J.; Ciais, P.; Deryng, D.; Folberth, C.; Hoek, S.; Izaurralde, R.; et al. The Global Gridded Crop Model Intercomparison phase 1 simulation dataset. *Sci. Data* **2019**, *6*, 50. [CrossRef]
7. USDA National Agricultural Statistics Service. Crop Progress Report. Available online: http://www.nass.usda.gov/Publications/National_Crop_Progress/ (accessed on 8 November 2021).
8. Zhang, X.; Friedl, M.A.; Schaaf, C.B.; Strahler, A.H.; Hodges, J.C.F.; Gao, F.; Reed, B.C.; Huete, A. Monitoring vegetation phenology using MODIS. *Remote Sens. Environ.* **2003**, *84*, 471–475. [CrossRef]
9. Zhang, X.; Liu, L.; Liu, Y.; Jayavelu, S.; Wang, J.; Moon, M.; Henebry, G.M.; Friedl, M.A.; Schaaf, C.B. Generation and evaluation of the VIIRS land surface phenology product. *Remote Sens. Environ.* **2018**, *216*, 212–229. [CrossRef]
10. Zeng, L.; Wardlow, B.D.; Wang, R.; Shan, J.; Tadesse, T.; Hayes, M.J.; Li, D. A hybrid approach for detecting corn and soybean phenology with time-series MODIS data. *Remote Sens. Environ.* **2016**, *181*, 237–250. [CrossRef]
11. Bolton, D.K.; Gray, J.M.; Melaas, E.K.; Moon, M.; Eklundh, L.; Friedl, M.A. Continental-scale land surface phenology from harmonized Landsat 8 and Sentinel-2 imagery. *Remote Sens. Environ.* **2020**, *240*, 111685. [CrossRef]
12. Taylor, S.D.; Browning, D.M.; Baca, R.A.; Gao, F. Constraints and Opportunities for Detecting Land Surface Phenology in Drylands. *J. Remote Sens.* **2021**, *2021*, 9859103. [CrossRef]

13. Gao, F.; Anderson, M.C.; Zhang, X.; Yang, Z.; Alfieri, J.G.; Kustas, W.P.; Mueller, R.; Johnson, D.M.; Prueger, J.H. Toward mapping crop progress at field scales through fusion of Landsat and MODIS imagery. *Remote Sens. Environ.* **2017**, *188*, 9–25. [CrossRef]
14. Diao, C. Remote sensing phenological monitoring framework to characterize corn and soybean physiological growing stages. *Remote Sens. Environ.* **2020**, *248*, 111960. [CrossRef]
15. Gao, F.; Zhang, X. Mapping Crop Phenology in Near Real-Time Using Satellite Remote Sensing: Challenges and Opportunities. *J. Remote Sens.* **2021**, *2021*, 8379391. [CrossRef]
16. Gao, F.; Anderson, M.; Daughtry, C.; Karnieli, A.; Hively, D.; Kustas, W. A within-season approach for detecting early growth stages in corn and soybean using high temporal and spatial resolution imagery. *Remote Sens. Environ.* **2020**, *242*, 111752. [CrossRef]
17. Liu, L.; Zhang, X.; Yu, Y.; Gao, F.; Yang, Z. Real-Time Monitoring of Crop Phenology in the Midwestern United States Using VIIRS Observations. *Remote Sens.* **2018**, *10*, 1540. [CrossRef]
18. Yan, L.; Roy, D.P. Conterminous United States crop field size quantification from multi-temporal Landsat data. *Remote Sens. Environ.* **2016**, *172*, 67–86. [CrossRef]
19. Gao, F.; Masek, J.; Schwaller, M.; Hall, F. On the blending of the Landsat and MODIS surface reflectance: Predicting daily Landsat surface reflectance. *IEEE Trans. Geosci. Remote Sens.* **2006**, *44*, 2207–2218. [CrossRef]
20. Gao, F.; Masek, J.G.; Wolfe, R.; Huang, C. Building a consistent medium resolution satellite data set using moderate resolution imaging spectroradiometer products as reference. *J. Appl. Remote Sens.* **2010**, *4*, 043526. [CrossRef]
21. Zhu, X.; Cai, F.; Tian, J.; Williams, T.K.-A. Spatiotemporal Fusion of Multisource Remote Sensing Data: Literature Survey, Taxonomy, Principles, Applications, and Future Directions. *Remote Sens.* **2018**, *10*, 527. [CrossRef]
22. Walker, J.J.; De Beurs, K.M.; Wynne, R.H.; Gao, F. Evaluation of Landsat and MODIS data fusion products for analysis of dryland forest phenology. *Remote Sens. Environ.* **2012**, *117*, 381–393. [CrossRef]
23. Zhang, X.; Wang, J.; Henebry, G.M.; Gao, F. Development and evaluation of a new algorithm for detecting 30 m land surface phenology from VIIRS and HLS time series. *ISPRS J. Photogramm. Remote Sens.* **2020**, *161*, 37–51. [CrossRef]
24. Claverie, M.; Ju, J.; Masek, J.G.; Dungan, J.L.; Vermote, E.F.; Roger, J.-C.; Skakun, S.V.; Justice, C. The Harmonized Landsat and Sentinel-2 surface reflectance data set. *Remote Sens. Environ.* **2018**, *219*, 145–161. [CrossRef]
25. Gray, J.; Sulla-Menashe, D.; Friedl, M. User Guide to Collection 6 MODIS Land Cover Dynamics (MCD12Q2) Product. Available online: https://lpdaac.usgs.gov/documents/218/mcd12q2_v6_user_guide.pdf (accessed on 8 November 2021).
26. Gao, F.; Anderson, M.C.; Hively, W.D. Detecting Cover Crop End-Of-Season Using VENμS and Sentinel-2 Satellite Imagery. *Remote Sens.* **2020**, *12*, 3524. [CrossRef]
27. Dedieu, G.; Hagolle, O.; Karnieli, A.; Ferrier, P.; Crébassol, P.; Gamet, P.; Desjardins, C.; Yakov, M.; Cohen, M.; Hayun, E. VENμS: Performances and first results after 11 months in orbit. In Proceedings of the 2018 IEEE International Geoscience and Remote Sensing Symposium (IGARSS 2018), Valencia, Spain, 22–27 July 2018. [CrossRef]
28. USDA National Agricultural Statistics Service. Quick Stats. Available online: https://quickstats.nass.usda.gov/ (accessed on 8 November 2021).
29. PhenoCam Network. Available online: https://phenocam.sr.unh.edu/webcam/ (accessed on 8 November 2021).
30. The Long-Term Agroecosystem Research (LTAR) Network. Available online: https://ltar.ars.usda.gov (accessed on 8 November 2021).
31. Browning, D.M.; Russell, E.S.; Ponce-Campos, G.E.; Kaplan, N.; Richardson, A.D.; Seyednasrollah, B.; Spiegal, S.; Saliendra, N.; Alfieri, J.G.; Baker, J.; et al. Monitoring agroecosystem productivity and phenology at a national scale: A metric assessment framework. *Ecol. Indic.* **2021**, *131*, 108147. [CrossRef]
32. Suyker, A.E.; Verma, S.B. Gross primary production and ecosystem respiration of irrigated and rainfed maize–soybean cropping systems over 8 years. *Agric. For. Meteorol.* **2012**, *165*, 12–24. [CrossRef]
33. Richardson, A.D.; Braswell, B.H.; Hollinger, D.Y.; Jenkins, J.P.; Ollinger, S.V. Near-surface remote sensing of spatial and temporal variation in canopy phenology. *Ecol. Appl.* **2009**, *19*, 1417–1428. [CrossRef] [PubMed]
34. Richardson, A.D.; Hufkens, K.; Milliman, T.; Aubrecht, D.M.; Chen, M.; Gray, J.; Johnston, M.R.; Keenan, T.; Klosterman, S.T.; Kosmala, M.; et al. Tracking vegetation phenology across diverse North American biomes using PhenoCam imagery. *Sci. Data* **2018**, *5*, 180028. [CrossRef] [PubMed]
35. European Space Agency (ESA). Sentinel-2 User Handbook. Available online: https://sentinels.copernicus.eu/documents/247904/685211/Sentinel-2_User_Handbook (accessed on 8 November 2021).
36. Roy, D.P.; Wulder, M.A.; Loveland, T.R.; Woodcock, C.E.; Allen, R.G.; Anderson, M.C.; Helder, D.; Irons, J.R.; Johnson, D.M.; Kennedy, R.; et al. Landsat-8: Science and product vision for terrestrial global change research. *Remote Sens. Environ.* **2014**, *145*, 154–172. [CrossRef]
37. The Harmonized Landsat-8 and Sentinel-2 (HLS) Data Product. Available online: https://hls.gsfc.nasa.gov/data/ (accessed on 8 November 2021).
38. USDA Farm Service Agency Handbook. Acreage and Compliance Determinations. Available online: https://www.fsa.usda.gov/Internet/FSA_File/2cp16-a1.pdf (accessed on 8 November 2021).
39. USDA National Agricultural Statistics Service. Iowa Crop Progress Reports. Available online: https://www.nass.usda.gov/Statistics_by_State/Iowa/Publications/Crop_Progress_&_Condition/ (accessed on 8 November 2021).
40. Boryan, C.; Yang, Z.; Mueller, R.; Craig, M. Monitoring US agriculture: The US Department of Agriculture, National Agricultural Statistics Service, Cropland Data Layer Program. *Geocarto Int.* **2011**, *26*, 341–358. [CrossRef]

41. USDA National Agricultural Statistics Service. Cropland Data Layer. Available online: http://www.nass.usda.gov/Research_and_Science/Cropland/SARS1a.php (accessed on 8 November 2021).

42. Appel, G. *Technical Analysis Power Tools for Active Investors*; Financial Times Prentice Hall: Upper Saddle River, NJ, USA, 2005; p. 166.

43. USDA National Agricultural Statistics Service. Usual Planting and Harvesting Dates for U.S. Field Crops. Available online: https://downloads.usda.library.cornell.edu/usda-esmis/files/vm40xr56k/dv13zw65p/w9505297d/planting-10-29-2010.pdf (accessed on 8 November 2021).

44. Iowa Environmental Mesonet. Available online: https://mesonet.agron.iastate.edu/ (accessed on 8 November 2021).

45. USDA Farm Service Agency. Crop Acreage Data. Available online: https://www.fsa.usda.gov/Assets/USDA-FSA-Public/usdafiles/NewsRoom/eFOIA/crop-acre-data/zips/2019-crop-acre-data/2019_fsa_acres_jan2020_stlno1.zip (accessed on 8 November 2021).

46. Houborg, R.; McCabe, M.F. A Cubesat enabled Spatio-Temporal Enhancement Method (CESTEM) Utilizing Planet, Landsat and MODIS Data. *Remote Sens. Environ.* **2018**, *209*, 211–226. [CrossRef]

47. Planet Lab Inc. Planet Fusion Monitoring Technical Specification. Available online: https://assets.planet.com/docs/Planet_fusion_specification_March_2021.pdf (accessed on 8 November 2021).

48. Cheng, Y.; Vrieling, A.; Fava, F.; Meroni, M.; Marshall, M.; Gachoki, S. Phenology of short vegetation cycles in a Kenyan rangeland from PlanetScope and Sentinel-2. *Remote Sens. Environ.* **2020**, *248*, 112004. [CrossRef]